CHAPTER 2

THE STATE OF THE OCEAN

This chapter includes an overview of the current state of knowledge about ocean climate, including anomalies, placed in historical context. Expert scientists who monitor, observe, and analyze the ocean products described in this chapter (e.g., sea level, ocean carbon, SST) have produced concise summaries describing why it is important to monitor these variables. Climate applications are presented along with an explanation of how the observing system needs to be enhanced to improve ocean analysis and reduce present uncertainties. This chapter focuses primarily on decision makers and non-scientists interested in, and concerned about, ocean research.

A performance measure is a structured statement describing how progress will be evaluated. Performance measures consist of four parts: indicator, unit of measure, baseline and target. An indicator defines the attribute or characteristic to be measured. The unit of measure describes what is to be measured. A baseline establishes the basis for comparison through an initial collection and analysis of data. A baseline should include both a starting date and level. A target establishes the desired level to be reached in a defined period, usually stated as an improvement over the baseline. Targets are based on research and a thorough understanding of the goal/program and are challenging, worthwhile and achievable (NOAA definition). A metric is any type of measurement used to gauge some quantifiable component of an agency's performance. Currently, the following performance measures exist for the ocean observation program.

<u>Present Performance Measure</u>:

1. Reduce the uncertainty in projections of *sea level rise* during the 21st century. Metric – the range between credible estimates of sea level rise (centimeters):

2002	2003	2004	2005	2006	2007	2008	2009	2010
80 cm	80 cm	70 cm	60 cm	50 cm	40 cm	30 cm	25 cm	25 cm

2. Reduce the uncertainty in estimates of the increase in *carbon inventory* in the global ocean. Metric – uncertainty in estimates of anthropogenic change per decade (Gigatons):

2002	2003	2004	2005	2006	2007	2008	2009	2010
10 Gt	10 Gt	10 Gt	8 Gt	8 Gt	7 Gt	6 Gt	4 Gt	4 Gt

3. Reduce the error in global measurement of sea surface temperature. Metric - Potential satellite bias error (degrees Celsius):

2002	2003	2004	2005	2006	2007	2008	2009	2010
0.7 C	0.7 C	0.6 C	0.5 C	0.4 C	0.3 C	0.2 C	0.2 C	0.2 C

The short articles presented in this chapter describe the products listed in Table 2.1 and are the result of ocean projects funded, in whole or in part, by NOAA's Office of Climate Observation.

Table 2.1. Products

2.1 Sea level to identify changes resulting from climate variability – *Laury Miller, Bruce Douglas, Robert Cheney*
2.2 Ocean carbon content every ten years and the air-sea exchange seasonally – *Rik Wanninkhof, Richard Feely*
2.3 Sea surface temperature to identify significant patterns of climate variability – *Richard Reynolds*
2.4 Surface currents to identify significant patterns of climate variability – *Peter Niiler, Nikolai Maximenko*
2.5 Sea surface pressure to identify changes in forcing functions driving ocean conditions and atmospheric conditions – *Ed Harrison*
2.6 Air-sea exchange of heat, fresh water, momentum to identify changes in forcing functions driving ocean conditions and atmospheric conditions – *Bob Weller*
2.7 Ocean heat and fresh water content and transports to identify where anomalies enter the ocean, how they move and are transformed, and where they re-emerge to interact with the atmosphere. Identify the essential aspects of thermohaline circulation and the subsurface expressions of the patterns of climate variability – *Lynne Talley*
2.8 El Niño and heat content variations – *Michael McPhaden*

2.1 GLOBAL SEA LEVEL RISE: THE PAST DECADE VS. THE PAST 100 YEARS

by Laury Miller[1], Bruce C. Douglas[2], Robert Cheney[1]

[1]Laboratory for Satellite Altimetry, NOAA/NESDIS, Silver Spring, MD
[2]Florida International University, Miami, FL

While "Climate Change" may seem a vague concept to some individuals, to the 100 million people who live within 1 meter of present day sea level, global sea level rise is anything but an abstraction, especially considering that sea level rose about 20 centimeters over the past century. How and why this change occurred, and whether the rate of global sea level rise (GSLR) is accelerating are questions of great interest to those directly threatened, to the governments and international bodies which ultimately will be called upon to deal with this issue, and to the public at large. And yet, it is important to note that the rate and causes of sea level rise are currently the subjects of intense scientific controversy.

The main elements of this controversy are documented in the climate assessment reports published periodically by the Intergovernmental Panel on Climate Change (IPCC). At the time of the second IPCC report in 1995, there seemed to be little dispute regarding GSLR. Most tide gauge estimates ranged between 1.5 to 2.0 mm/year. Most of this rise was thought to be due to ocean warming causing the volume of the oceans to increase, with the rest due to the melting of continental ice, primarily in Greenland and Antarctica, causing the mass of the oceans to increase. However, by the time of the 2001 IPCC assessment, this consensus view had collapsed. New and better estimates of ocean warming had reduced the volume component of GSLR to about 0.5 mm/year and the mass component was thought to be even smaller. This left a large unexplained gap between direct and indirect estimates of GSLR that has come to be known as the "attribution problem". Either the gauge estimates are too high, or one (or both) of the mass and volume change estimates is too low.

Two recent studies offer opposing solutions to this dilemma. Cabanes et al. (2001) argue that tide gauge measured rates of GSLR are 2 to 3 times too high because the gauges happen to be located in areas of abnormally high ocean warming. They arrive at this result by comparing gauge measured sea level trends with those obtained from objectively interpolated temperature and salinity measurements. They conclude that the true rate of GSLR is actually 0.5 to 1.0 mm/year, due mostly to ocean warming. This solution provides a way out of the attribution problem, but implies a huge acceleration of GSLR in the 1990's if recent satellite altimetric estimates of ~2.5 mm/year are to be believed.

Alternately, Antonov et al. (2002) suggest that the problem may be solved by revising upward the mass component estimate. They show that the oceans are freshening at a rate equivalent to the addition of 1.4 mm/year of fresh water, approximately the amount needed to bring the mass plus volume rate close to the tide gauge measured rate. However, this solution assumes a continental ice source rather than floating ice, a key point that they are unable to demonstrate.

In the latest chapter of this debate, Miller and Douglas (2004) have re-examined the tide gauge bias issue on a regional as well as local scale. They identify large ocean areas that are either bounded by or adjacent to several gauge sites exhibiting similar trends and variability. For those areas they compare average gauge measured sea level trends with the trends computed from actual rather than interpolated measurements of temperature and salinity.

Figure 1 presents an example of their analysis for a region in the Eastern Pacific bounded by the gauges at Honolulu, San Francisco, San Diego, and Balboa, Panama. All four gauge records

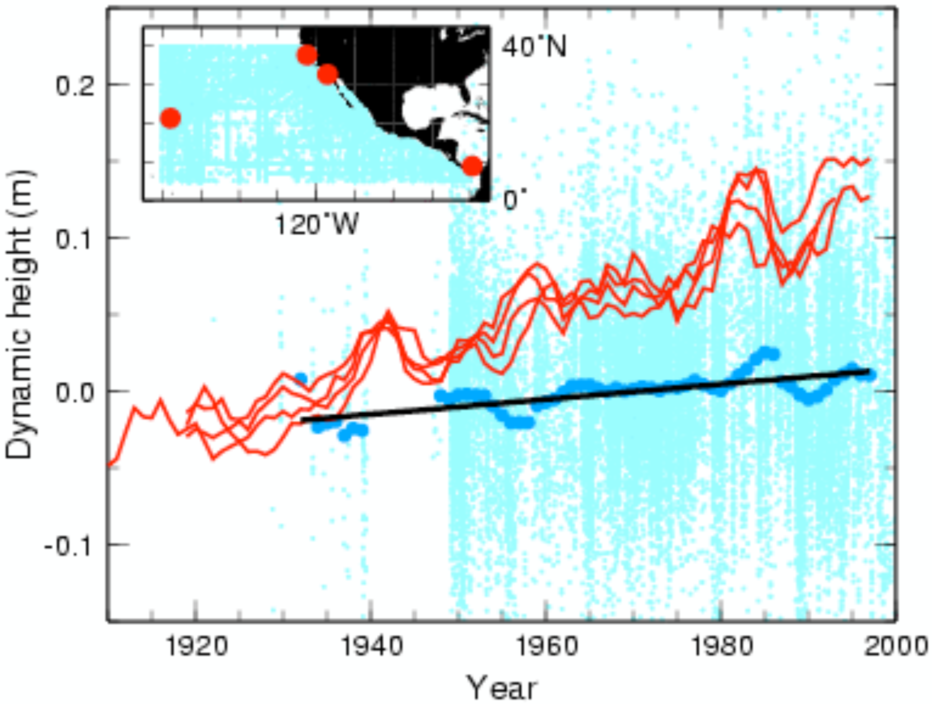

Figure 1. Eastern Pacific hydrographic observations of temperature and salinity converted into 1000 m dynamic height anomalies (light blue), their 5 year running means (dark blue) and linear regression (black) compared with 5 year running mean relative sea levels from tide gauge observations at San Francisco, San Diego, Honolulu, and Balboa (red). Tide gauge series have been vertically offset to coincide with earliest dynamic heights. Map inset shows tide gauge locations in red and observed dynamic height locations in light blue (Miller and Douglas, 2004).

show sea-level trends of about 2 mm/year during the 20th century, despite the fact that the gauge sites are widely separated and, thus, subject to different vertical land motions and local hydrographic conditions. However, the ~19,000 hydrographic stations from the ocean interior show that only about 0.5 mm/year of sea-level rise can be accounted for by temperature and salinity changes.

Limiting this analysis to small areas immediately adjacent to the gauge sites gives essentially the same results. Locally, only a fraction of the gauge-measured sea level rise is the result of hydrographic (volume) changes. One conclusion of this study is that the gauges are not situated in regions of abnormally high warming. Thus, gauge estimates of 1.5 to 2.0 mm/year for 20th century GSLR are probably correct. Another, perhaps more surprising conclusion is that the melting of continental ice sheets and glaciers plays a more important role in GSLR than ocean warming.

While the debate over 20th century GSLR will no doubt continue, the question of whether the present rate of GSLR differs from the 20th century rate is beginning to attract attention because of the recent availability of satellite altimeter observations of sea level rise. Unlike tide gauge data, which are geographically sparse and require a long (50 to 75 year) averaging interval to filter out interdecadal variability, satellite altimeter data have the advantage of dense, global coverage and are beginning to offer, in a relatively short time, new insights into the GSLR problem.

For example, Figure 2 presents global sea level time series from the six satellite altimeters that operated from 1992 onward. Each record trends upward, with a group average rate of about 2.4 mm/year. The TOPEX/Jason series, considered the most accurate of the group, give a rate of about 2.8 mm/year. Whether either of these values reflects a true acceleration with respect to the 20th century tide gauge-derived rate or is simply evidence of decadal variability is unclear at this time. The 1990's were a period of exceptional warming events in the ocean. In addition to intense ENSO variability in the tropics, there is evidence from both altimeter and *in situ* hydrographic measurements of strong regional warming at mid-latitudes in the southern hemisphere which may account for as much as 1.8 mm/year of global rise between 1993 and 2002 (Willis et al., 2004). It is thought that 15 to 20 years of continuous altimeter measurements may be needed to obtain a stable value for the current rate of GSLR. They also highlight the importance of in-situ observing systems, like the NOAA-supported tide gauge network and ARGO profiling array, to validate the altimeter results and provide information on the internal structure of the oceans essential to understanding the processes governing GSLR.

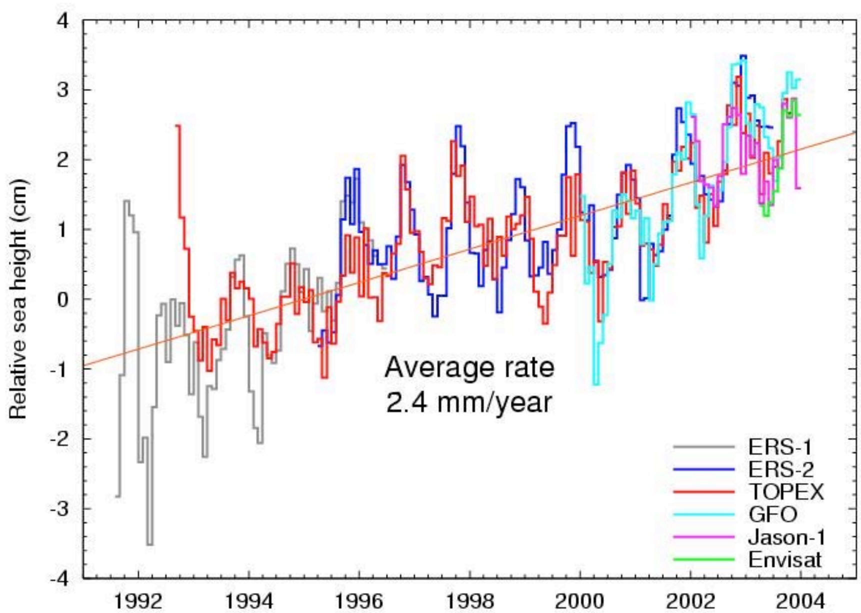

Figure 2. Global sea level rise determined over the past decade by TOPEX/Poseidon, Jason, Geosat Follow-on, ERS-1 and 2 satellite altimeters. After removing respective biases, the general trend is approximately 2.4 mm/year.

References

Antonov, J. I., S. Levitus, and T. P. Boyer, Steric sea level variations 1957-1994: importance of salinity, *Journal of Geophysical Research, 107*, 12, 8013, 2002.

Cabanes, C., A. Cazenave, and C. LeProvost, Sea level rise during past 40 years determined from satellite and *in situ* observations, *Science*, *294*, 840-842, 2001.

Miller, L. and B. C. Douglas, Mass and volume contributions to 20th century global sea level rise, *Nature,* in press, 2004.

Willis, J., D. Roemmich and B. Cornuelle, Intrannual variability in upper-ocean heat content, temperature and thermosteric expansion on global scales, *Journal of Geophysical Research*, submitted, 2004.

2.2 OBSERVING THE GLOBAL OCEANIC CARBON CYCLE

by Rik Wanninkhof[1] and Richard Feely[2]

[1]Atlantic Oceanographic and Meteorological Laboratory, Miami, Florida
[2]Pacific Marine Environmental Laboratory, Seattle, Washington

The Global Carbon Cycle: Inventories, Sources and Sinks
Carbon dioxide is one of the major greenhouse gases, contributing about 60% of the total change in radiative forcing due to human perturbations (Houghton et al. IPCC, 2001). The total emission due to fossil fuel use and cement production averaged about 6.3 ± 0.4 Pg C per year in the 1990s (1 Pg C = 1 peta gram carbon = 10^{15} gram = 1 gigaton). Although this annual CO_2 release has an appreciable effect on the earth radiation balance, it is a small fraction of the reservoir sizes comprising less than 1% of the CO_2 in the atmosphere, 0.3% of the labile terrestrial carbon pool; and 0.02% of the total carbon content of the ocean. The annual addition is also much smaller than the natural exchanges between the reservoirs comprising less than 10% of the natural annual exchanges between ocean and atmosphere, and between the terrestrial biosphere and atmosphere. The reservoir sizes and exchanges between reservoirs on an annual basis are shown in Figure 1.

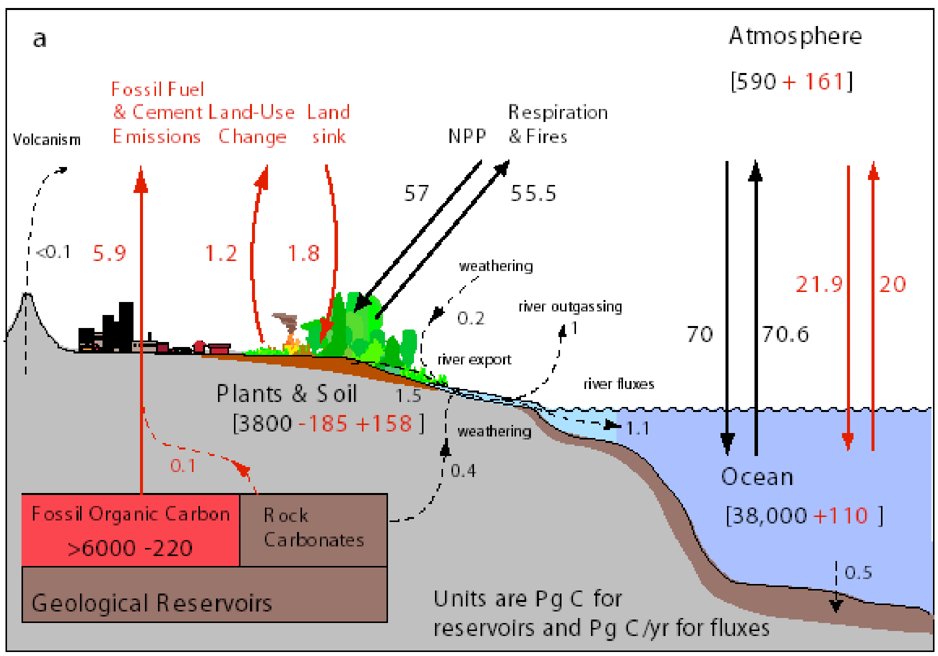

Figure 1. Cartoon of fluxes (arrows) and inventories (number in boxes) of the labile components of the global carbon system for the 1980s. The red arrows are the perturbation fluxes resulting from emissions of anthropogenic CO_2. From Sabine et al. (2003).

Although the anthropogenic perturbation seems small compared to the natural cycling of carbon between ocean, atmosphere and terrestrial systems, models and observations suggest that the increasing CO_2 levels in the atmosphere are causing an increase in global temperature (Fig. 2). While the evidence is rapidly growing for a causal relationship, it has not been unambiguously established yet. The perturbation is also showing effects on terrestrial and oceanic ecosystems.

Based on carbon and carbon isotopic records in ice cores and tree rings we know that the atmospheric CO_2 levels remained very constant at 280 ± 5 parts per million (ppm) for the millennium prior to the industrial revolution. The remarkable constancy of atmospheric CO_2

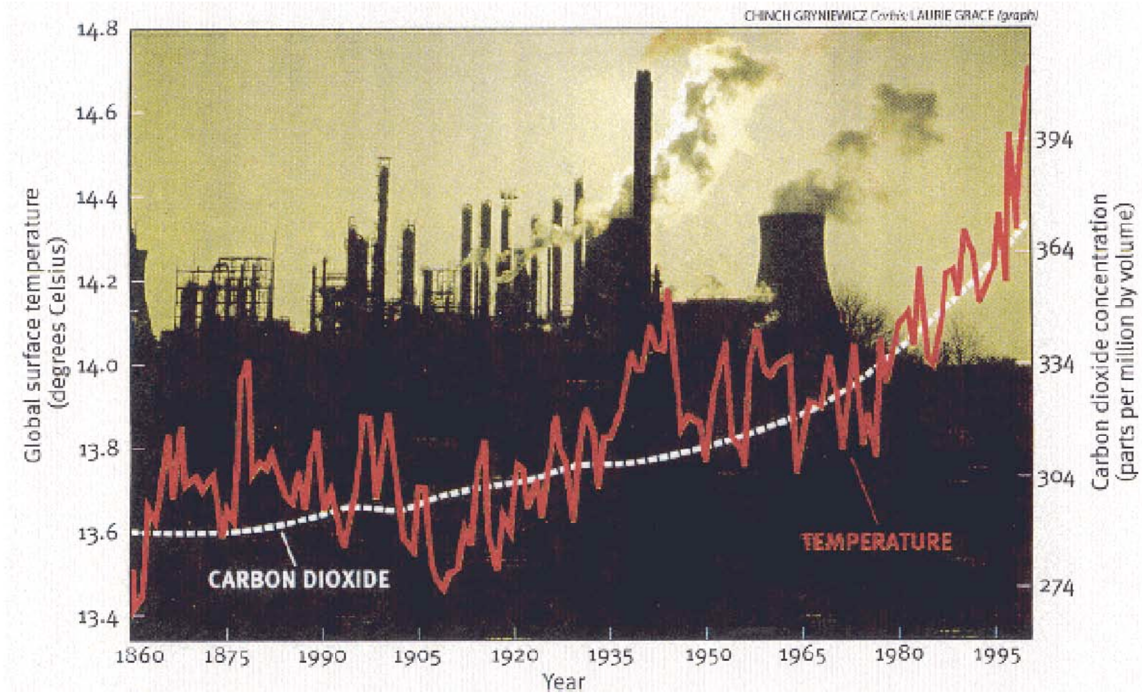

Figure 2. Trends of atmospheric carbon dioxide levels (white dashed line, right axis) and global surface temperature (red dashed line).

despite large exchanges between the major reservoirs suggests a well-balanced global carbon cycle prior to the Industrial Revolution. However, we also know from the paleo-records that atmospheric CO_2 levels varied in proportion to global temperatures between ice ages and warmer periods. Therefore, it seems quite possible that the current dramatic atmospheric CO_2 level rise will have a significant effect on climate and ecosystems. Moreover, although we have good paleo-records of climate in low CO_2 environments we have very limited information of how the earth responds to the current unprecedented high CO_2 levels and anticipated increases in the next century.

Our current knowledge of the fate of the anthropogenic CO_2 released to the atmosphere is based on models; atmospheric observations of CO_2, carbon isotopes and small decreases in oxygen levels; terrestrial measurement of biomass inventories and primary productivity; and oceanic measurements of CO_2 inventories and fluxes between air and ocean. Less than a decade ago there were significant discrepancies between estimates leading to the popular notion of the "missing carbon sink". There now is broad agreement that the "missing sink" is uptake by the terrestrial ecosystems based on disparate methods as summarized in Table 1.

As the table indicates, our level of confidence in different observations ranges from a general good knowledge of the annual changes in some reservoirs, to highly uncertain estimates in others. Annual releases due to fossil fuel burning and cement production, and annual atmospheric CO_2 increases are the most constrained. Decadal changes in the ocean carbon inventory have recently been established with reasonable confidence. Changes in the terrestrial biosphere have been more difficult to pinpoint. From a variety of observations we now have a reasonable estimate of the partitioning of the fossil fuel carbon between reservoirs over the last two centuries with roughly 50% ending up in the ocean. The terrestrial systems released CO_2 over this same period. Over the last two decades, however, the terrestrial systems appear to have taken up CO_2 but the

Table 1. Global inventory of anthropogenic CO_2 for the past 200 and 20 years

CO_2 Sources	1800-1994 [Pg C][a]		1980-1999 [Pg C][g]
Constrained sources and sinks			
(1) Emissions from fossil fuel and cement production	244 [(b)]	± 20	117±5
(2) Storage in the atmosphere	-165 [(c)]	± 4	-65±1
(3) Uptake and storage in the ocean	-118 [(d)]	± 19	-37±8
Inferred net terrestrial balance			
(4) Net terrestrial balance = [-(1)-(2)-(3)]	39	± 28	-15±9
Terrestrial balance			
(5) Emissions from land use change	100 to 180[(e)]		24±12
(6) Terrestrial biosphere sink = [-(1)-(2)-(3)]-(5)	-61 to -141		-39±18

From Sabine et al., 2004

magnitude, cause, and particularly the longevity of this sink remains in great doubt. Significant efforts, such as those proposed in the North American Carbon Plan (NACP), are underway to directly determine CO_2 sources and sinks in the terrestrial system. However, in the foreseeable future the best approach for constraining the net terrestrial flux will be from the difference between atmospheric and oceanic observations and model calculations.

The need for an integrated investigation of the carbon cycle has been well articulated in the US Carbon Cycle Science Plan (Sarmiento and Wofsy, 1999). Through efforts of the Interagency Carbon Working Group and the Scientific Advisory Committee, science and implementation plans have been developed for subcomponents of the program including the NACP Science Plan, the NACP Implementation Strategy, the Ocean Carbon and Climate Change Implementation Strategy, and the Large Scale Carbon Observing Plan (LSCOP) (Bender et al., 2001). The LSCOP plan in particular focuses on the implementation and justification for sustained ocean observations. All of the plans address the central tenets of the Carbon Cycle Science Plan, which focuses on the "excess carbon", that is the carbon produced by fossil fuel burning and other activities of mankind releasing CO_2 such as land use change:

- Where has the excess carbon gone to over the last two centuries?

- Where will the excess carbon go to in the future?
- What processes are involved in sequestration of the excess carbon?
- Can the future sinks be managed and increased?

Because of the sensitivity of the global economy to terrestrial and oceanic ecosystems, and regional climate, the issue of carbon accounting transgresses the usual stakeholders of scientific information. Like emissions of pollutants, carbon emissions now have an economic value. The number $40 per metric ton carbon sequestered is often used in estimates. Improved constraints on the carbon sources and sinks can now be directly translated into a currency equivalent. For instance, the global uptake of carbon by the ocean of about 1.6 Pg C yr^{-1} (Table 2) translates into a $64 billion service to the global economy. As shown in Table 2, the uncertainty in the ocean sink is significant translating into an uncertainty in the value of this commodity. Knowledge of the future sink strength of the ocean is thus critical from scientific and economic perspective.

Table 2. Summary of estimated global CO_2 fluxes using different gas transfer velocities but the same ΔpCO_2 climatology.

Parameterization	Uptake (Pg C/yr)
Wanninkhof, 1992	-1.6
Wanninkhof and McGillis, 1999	-1.9
Nightingale, 2000	-1.2
Liss and Merlivat, 1983	-1.0

All these values were obtained using the ΔpCO_2 climatology of Takahashi et al. (2002) and 41-year climatological 6-hour winds from the NCAR/NCEP reanalysis project. The divergence of values illustrates that besides determining seasonal ΔpCO_2 fields the gas transfer velocity needs to be better constrained.

References for the relationships:

Liss, P.S., and L. Merlivat, Air-sea gas exchange rates: Introduction and synthesis, in *The Role of Air-Sea Exchange in Geochemical Cycling*, edited by P. Buat-Menard, pp. 113-129, Reidel, Boston, 1986.

Nightingale, P.D., G. Malin, C.S. Law, A.J. Watson, P.S. Liss, M.I. Liddicoat, J. Boutin, and R.C. Upstill-Goddard, *In situ* evaluation of air-sea gas exchange parameterizations using novel conservative and volatile tracers, *Global Biogeochemical Cycles*, *14*, 373-387, 2000.

Wanninkhof, R., Relationship between gas exchange and wind speed over the ocean, *Journal of Geophysical Research*, *97*, 7373-7381, 1992.

Wanninkhof, R., and W.M. McGillis, A cubic relationship between gas transfer and wind speed, *Geophysical Research Letters*, *26*, 1889-1893, 1999.

The Sustained Ocean Component of the Carbon Cycle Science Plan

The oceanic carbon-observing program addresses two important subcomponents of the determination of the fate of the excess CO_2 in the ocean:

- Determining oceanic carbon inventories and attributing the cause of the variations in inventories over time
- Quantifying the air-sea CO_2 fluxes and creating of seasonal flux maps

Ocean inventories

As a result of the measurements during the global CO_2 survey in the 1990s and improved methods of quantifying the anthropogenic CO_2 signal above the large natural background, we now have the first measurement based inventory of anthropogenic CO_2 in the ocean. The excess CO_2 has been gridded at 1 degree spacing and 33 levels so it can be compared directly with model outputs. The observations show that surface waters are in near equilibrium with the atmospheric rise with a perturbation of the total carbon content of about 3% (60 μmol kg^{-1} out of a natural background of 2000 μmol kg^{-1}). The anthropogenic inventory decreases rapidly with depth for most parts of the ocean. Characteristic cross sections for the Atlantic, Indian and Pacific basins are shown in Figure 3. The distribution closely follows the known ventilation pathways of the ocean with deep penetration in the North Atlantic and storage of much of the carbon in the mid-latitude convergence zones. The total uptake over the past 200 years shown in Table 1 validates the model estimates. The total inventory is similar to models but the regional inventory is quite different suggesting that most of the models do not adequately capture the processes responsible for uptake at regional scales.

Decadal inventory changes

The measurement based total inventory of anthropogenic carbon in the ocean is a critical constraint for models and for our understanding of the role of the ocean in the sequestration of excess carbon. However, information on shorter timescales is essential to determine any feedbacks of oceanic carbon sequestration due to climate change, and to determine the role of natural variability on the oceanic carbon system. Therefore the COSP has started, in collaboration with NSF and NASA, a repeat hydrography program. The main objective of the repeat hydrography component of the sustained ocean observing system for climate is to document long-term trends in carbon storage and transport in the global oceans. This program will provide composite global ocean observing system large-scale observations that include: 1) detailed basin-wide observations of CO_2, hydrography, and tracer measurements; and 2) data delivery and management. This repeat hydrography program will provide the critical and timely information needed for climate research and assessments, as well as long-term, climate quality, global data sets.

The first three cruises of the repeat hydrography program were completed in 2003 focusing on the North Atlantic to provide a constraint for the NACP program. The initial highlights are that the ventilation pattern/circulation in the North Atlantic thermocline has changed based on a significant change in oxygen content (Fig. 4). Also, we have been able to unambiguously determine an increase in total carbon content in the upper ocean over 6 to 10 years suggesting that uptake of anthropogenic CO_2 continues unabated and that we can detect anthropogenic carbon increase in the ocean on decadal timescales. (Fig. 5)

Atmosphere-Ocean CO_2 Fluxes

Background

Changes in carbon inventory are the most robust means of assessing sources and sinks but for the oceans these methods are limited to changes over decadal timescales. On average the total dissolved inorganic carbon content (DIC) of the surface ocean increases by about 1 μmol kg^{-1} per year or about 0.05% over the background. While the accuracy of DIC measurements is about 2 μmol kg^{-1} making detection of the anthropogenic signal in principle possible on shorter time

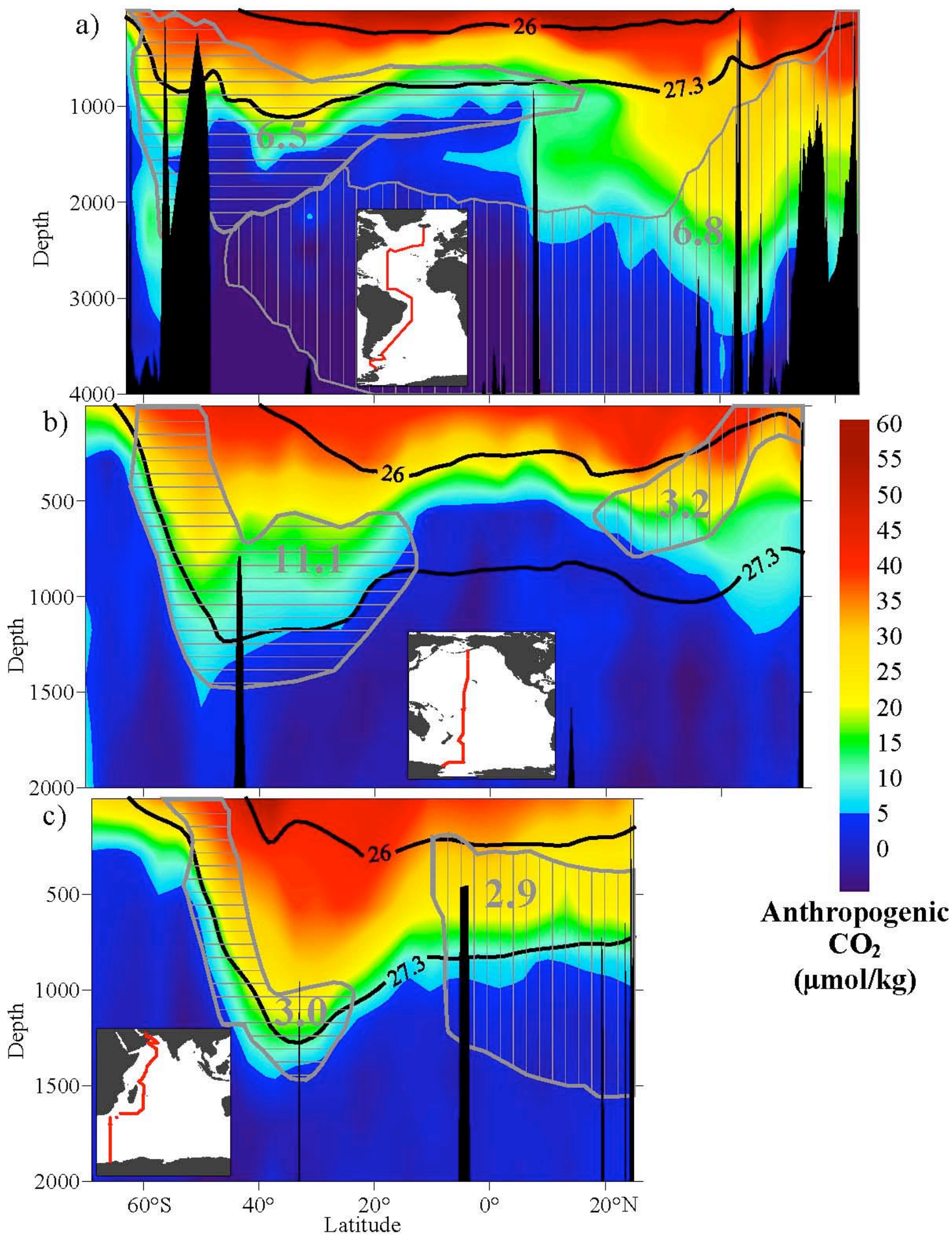

Figure 3. Representative sections of anthropogenic CO_2 (µmol kg^{-1}) from the Atlantic (a), Pacific (b) and Indian (c) Oceans. Grey hatched regions and numbers indicate amount of anthropogenic carbon stored (Pg C) in the intermediate water masses. The two heavy lines on each section give the characteristic potential density contours for the near surface water and intermediate water. Much of the penetration of anthropogenic carbon into the ocean follow isopycnal surfaces. From Sabine et al. (2004).

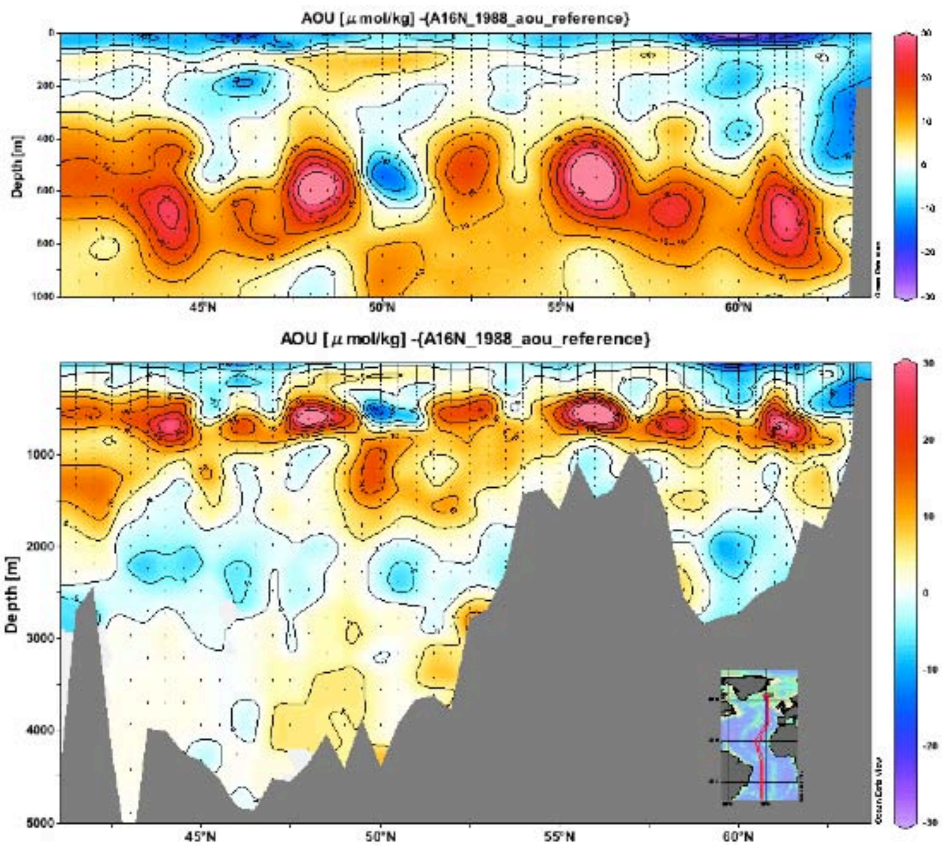

Figure 4. Distribution of the apparent oxygen utilization (AOU) difference between 2003 – 1988 (μmol kg^{-1}) in the North Atlantic Ocean along 20˚W. The large differences between 400 – 800 m in the water column corresponds to changes in oxygen content of over 20% at these depths (preliminary data provided by J. Bullister, PMEL).

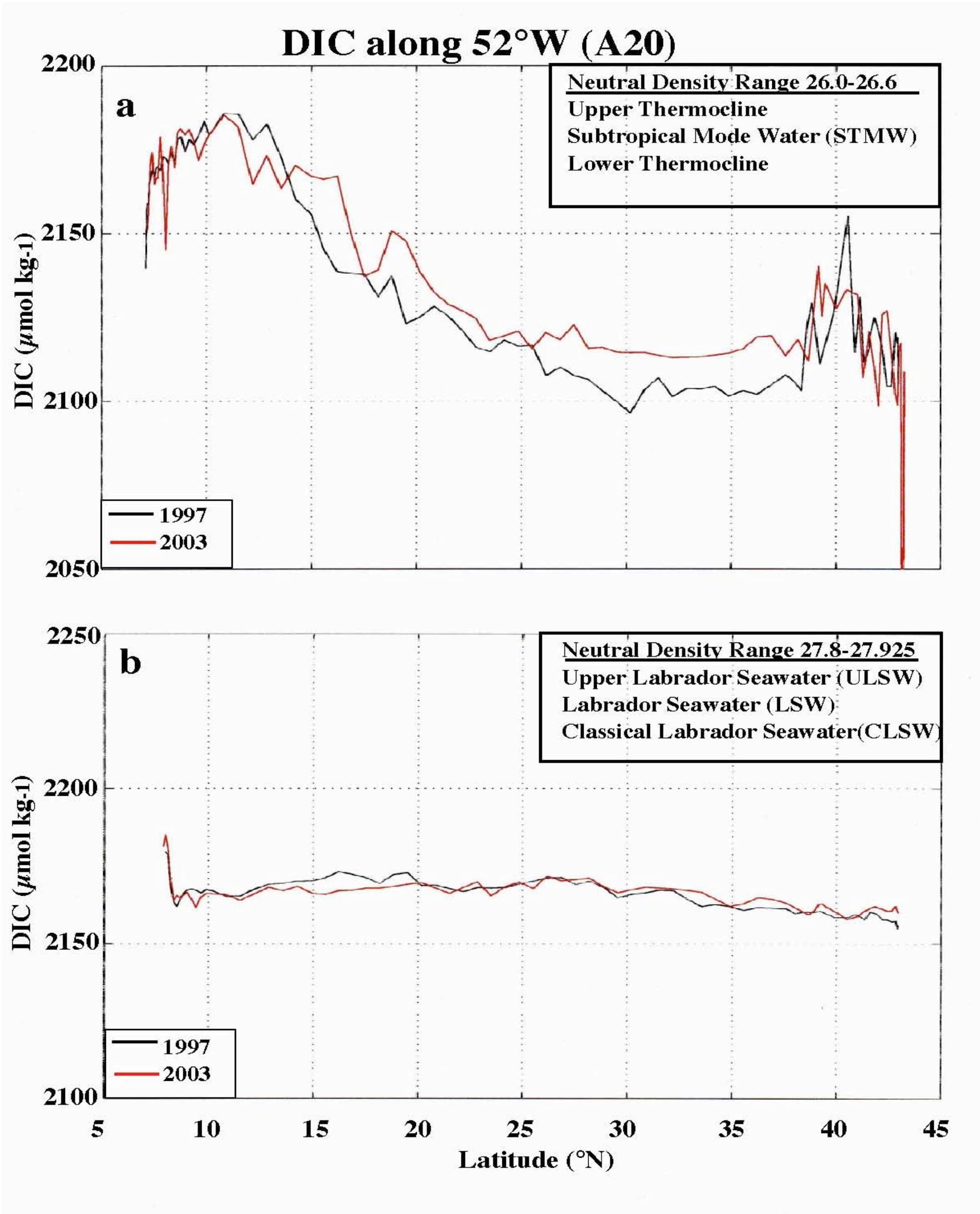

Figure 5. Comparison of the total dissolved inorganic carbon concentrations, DIC concentrations a) near the surface (in the density range of 26.0 – 26.6); and b) for the 27.80 – 27.93 isopycnals for 1997 and 2003 in the western North Atlantic. (based on preliminary data from M. Roberts-Lamb, PMEL)

scales, the surface ocean DIC changes by 20 to 50 μmol kg^{-1} seasonally masking changes less than 5 to 10 μmol kg^{-1}.

To assess changes in exchanges between reservoirs on sub-decadal timescale we have to determine the fluxes. The fluxes can be determined from measuring the partial pressure differences of CO_2 between surface ocean and lower atmosphere, ΔpCO_2, and a quantity referred to as the gas transfer velocity that is related to physical forcing and often parameterized with wind speed. Thus, if ΔpCO_2 fields can be determined and used in combination with wind fields, regional fluxes can be obtained.

Creation of flux maps

This approach has been applied successfully using a global climatology of ΔpCO_2 painstakingly developed based on 40-years of ΔpCO_2 data from many investigators (Takahashi et al., 2002). Uptakes based on this climatology range from 1 to 1.9 Pg C yr^{-1} depending on the relationship between gas exchange velocity and wind speed (Table 2). This approach will be used to quantify regional fluxes on a seasonal timescale. The implementation will require a significant increase in ΔpCO_2 observations, development of methods to interpolate ΔpCO_2 in time and space, and improvement of algorithms to quantify the gas transfer from wind or other relevant parameters, such as surface roughness, that can be directly observed from remote sensing.

Following a recommendation in the LSCOP plan a surface ocean flux observing system is being put in place with autonomous instrumentation on volunteer observing ships VOS, research ships, and buoys. The LSCOP plan lays out an observing strategy based on scaling analysis that involves sampling of the ocean roughly at 10 degree spacing and monthly intervals. By coordinating efforts with international and national partners this goal will be attainable in the next decade for the North Atlantic, North Pacific and Equatorial Pacific, particularly if we develop methods to increase time and space scales of observation through use of remotely sensed observations. The scheme of implementing such a system utilizing *in situ* and remotely sensed data is outlined in Figure 6.

Determining and attributing changes in ΔpCO_2

The approach of utilizing remote sensing, algorithms of ΔpCO_2 and gas exchange with remotely sensed products has been utilized in test beds in the Equatorial Pacific and Caribbean Sea. Flux map products for these regions are shown in Figures 7 and 8. For the Equatorial Pacific work the algorithms are used in a retrospective fashion to determine the large variations in air-sea flux due to the ENSO Cycle.

Limited time series records of surface water pCO_2 levels have shown that for much of the ocean the surface water pCO_2 rises roughly at the same rate as the atmospheric increase implying that the global air-sea flux remains the same. However, changes in the rate of increase are a sensitive indicator of changes in the uptake of the ocean and perturbations in the biogeochemical cycles. Using a historical database of ΔpCO_2 for the Equatorial Pacific Takahashi et al. (2003) determined significantly slower increases in the 80s than in the 90s that were attributed to a climatic re-organization in the North and Equatorial Pacific referred to as the Pacific Decadal Oscillation (PDO).

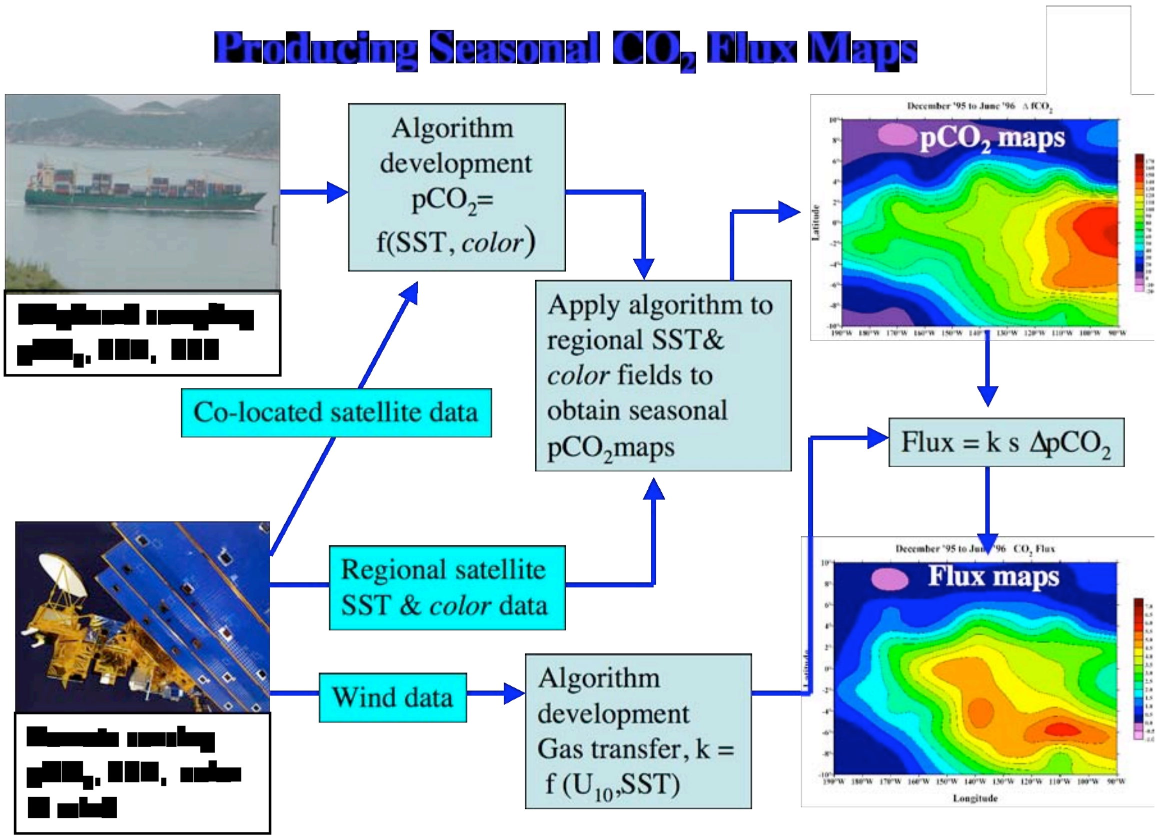

Figure 6. Flow diagram of data and procedures to produce pCO_2 flux maps.

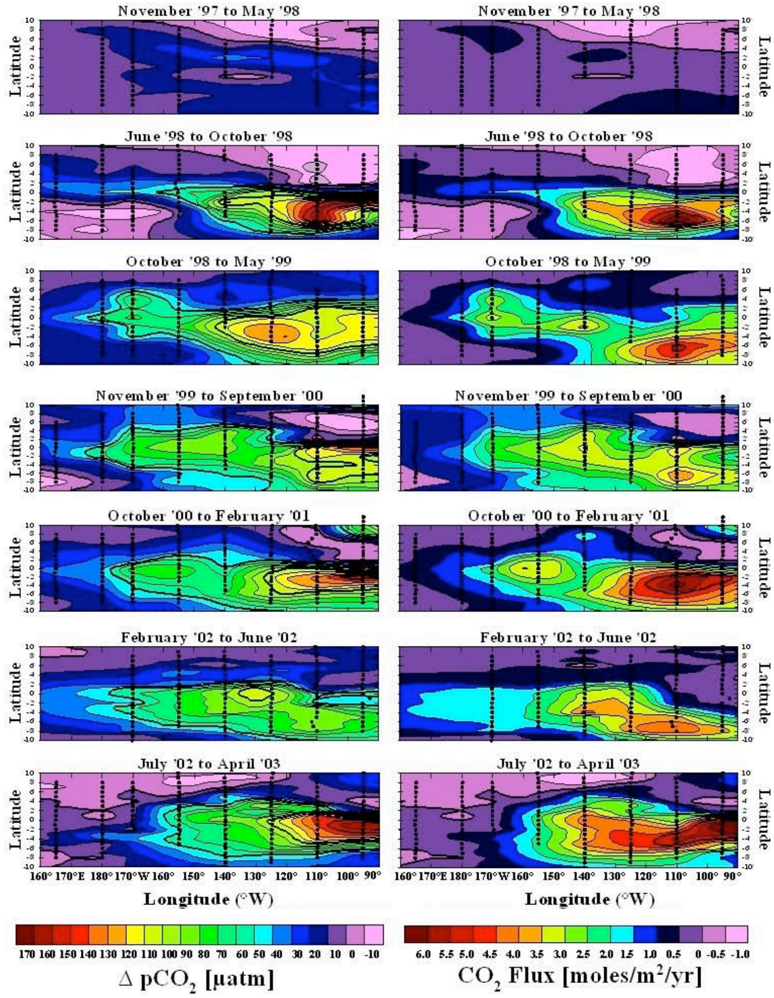

Figure 7. Maps of ΔpCO_2 (left) and CO_2 fluxes in moles m^{-2} yr^{-1} in the equatorial Pacific from November 1997 thru April 2003 based on *in situ* observations and remotely sensed winds and sea surface temperature. The higher pCO_2 values and normal winds in the eastern Pacific during the 2002-03 El Niño event led to unusually high sea-to-air CO_2 fluxes for an ENSO event. After Feely et al. (2002).

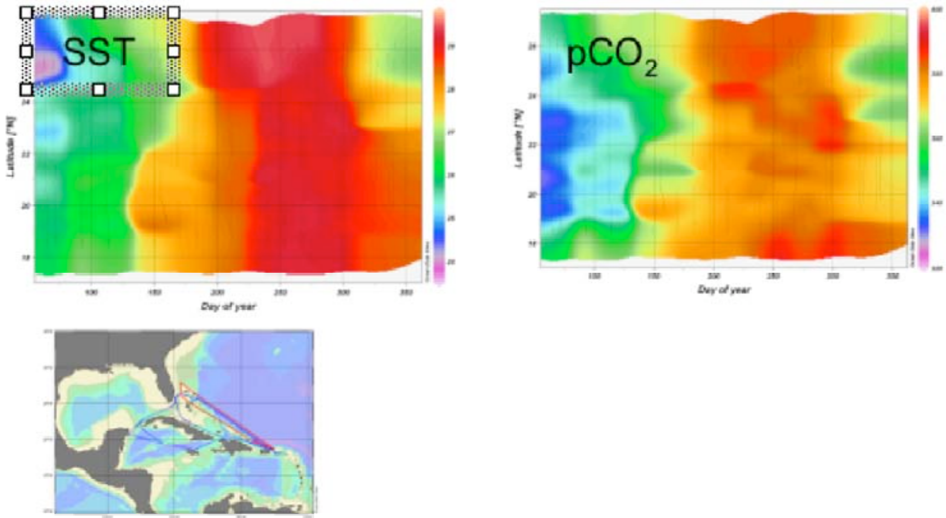

Figure 8. Production of pCO_2 maps in the Caribbean. Empirical algorithms are being developed with parameters that are measured at higher density/frequency (e.g., through remote sensing). The close correspondence of temperature (left panel) trends and pCO_2 (right panel) along the cruise track (bottom) facilitates robust algorithms to extrapolate the pCO_2 to regional scales. From Olsen et al. (2004).

Future plans and milestones

The observational efforts to detect changes in water column inventories and to attribute the causes, and the development of regional CO_2 flux maps are part of well documented and justified integrated carbon plans. The CO_2/CLIVAR Repeat Hydrography Program has a series of cruises planned for the next decade that will yield sequential basin wide inventory changes for the Atlantic, Pacific, Southern and Indian oceans. The cruise sequence is listed in Table 3. NOAA/COSP has the lead on the cruises for A16S, A16N, P16N, P18 and I8. NOAA participants will perform DIC and pCO_2 measurements on all cruises. Operational Milestones are provided in Table 4.

Table 3. Schedule of the repeat hydrography transects

Schedule of US CO2/CLIVAR Hydrography Lines (as of 4/25/03)

Dates	Cruise	Days	Ports	Year	Contact/Chief Scientist
					overall coordinator: Jim Swift, SIO
6/19/03-7/10/03	A16N, leg 1	22	Reykjavik-Madeira	1	Bullister, PMEL
7/15/03-8/11/03	A16N, leg 2	28	Madeira - Natal, Brazil	1	Bullister, PMEL
9/15/03-10/13/03	A20	29	WHOI - Port Of Spain	1	Toole, WHOI
10/16/03-11/07/03	A22	21	Port Of Spain - WHOI	1	Joyce, WHOI
summer 2004	P2 (two legs)	66	San Diego-Honolulu-Yokohama	2	Swift/Robbins, SIO
austral summer 05	A16S	44	Montevideo-Fortaleza Brazil	3	
austral summer 05	P16S	40	Wellington-Tahiti	3	
2006	P16N	57	Tahiti-Alaska	4	
austral summer 07	S4P/P16S	25.5	Wellington-Perth	5	
austral summer 07		25.5	Wellington-Perth	5	
2008	P18	32	Punta Arenas-Easter Island	6	
2008		35	Easter Island- San Diego	6	
2008	I6S	42	Cape Town	6	
2009	I7N	47	Port Louis/Muscat	7	future planning
2009	I8S	38	Perth- Perth	7	future planning
2009	I9N	34	Perth- Calcutta	7	future planning
2010	I5	43	Perth - Durban	8	future planning
2010	A13.5	62	Abidjan-Cape Town	8	future planning
2011	A5	30	Tenerife-Miami	9	future planning
2011	A21/S04A	42	Punta Arenas-Cape Town	9	future planning
2012	A10	29	Rio de Janeiro-Cape Town	10	future planning
2012	A20/A22	29	Woods Hole-Port of Spain-Woods Hole	10	future planning

Years 1-6 are funded.

Table 4. Operational milestones of the CO_2/CLIVAR Repeat Hydrography Program

Summer 2003	Organize and complete the A16N cruise in the North Atlantic and provide leadership (chief scientist), CTD, oxygen, nutrient, total carbon and pCO_2 analysis
Winter 2003/2004	Provide final CO_2, oxygen, CTD data to the repeat hydrography data center at Scripps
Summer 2004	Analyze total inorganic carbon on the P2 cruise
Winter 2004/2005	Provide final total CO_2 data to the repeat hydrography data center at Scripps
Winter 2004/2005	Organize and complete the A16N cruise in the North Atlantic and provide leadership (chief scientist), CTD, oxygen, nutrient, total carbon and pCO_2 analysis
Winter 2004/2005	Analyze total inorganic carbon on the P16S cruise
Spring 2006	Organize and complete the P16N cruise in the Pacific and provide leadership (chief scientist), CTD, oxygen, nutrient, total carbon and pCO_2 analysis

The COSP CO_2 flux map effort focuses on the ΔpCO_2 observations needed to create the seasonal maps. The initial lines in the North Atlantic are shown in Figure 9. The implementation schedule is presented in Table 5 with the italicized text that will be proposed in FY 05. The effort is starting to incorporate time series on moorings that are critical to determine the higher frequency (< 1 month) temporal variability. Particularly in the coastal oceans and Equatorial Pacific large changes can occur on weekly timescales. The exact balance and number of fixed pCO_2 observing sites vs. ship-based (moving) observing platform has not been firmly established. Analysis of the results of the initial surface pCO_2 observing system will be used to optimize spacing, frequency, and mix of observing methods. Optimizing the observing system requires inclusion of measurements of biogeochemical and physical parameters that influence pCO_2 as well in order to investigate extrapolation routines. The added benefit will be that these parameters yield mechanistic information that can be used in prognostic models and interpolation schemes utilizing satellite data. An end-to-end iterative effort starting from observations to interpretation and analysis feeding into improved observing system design and assessing the state of the ocean carbon cycle is critical at this point and attainable within national and international frameworks.

National and International Linkages

The COSP carbon program is an integral part of national and international programs in carbon cycle research. NOAA's contribution is unique as it is the only program that has the sustained observational effort necessary to constrain sources and sinks and provide input for prognostic models to predict future trends. The international connection for the repeat hydrography effort is through WCRP/CLIVAR and the IGBP/IMBER programs. The former is focused on the physical aspects of climate variability while the latter is geared to the ecological and biogeochemical components. The flux map effort is connected to the SOLAS effort theme 3: Air-Sea Flux of CO_2 and Other Long-Lived Radiatively-Active Gases. International coordination for both aspects of CO_2 COSP will occur through the International Ocean Carbon Co-ordination Project (IOCCP). International ties between the ocean carbon programs and the atmospheric, terrestrial, and human dimension carbon cycle research are provided through the IGBP/WCRP/IHDP Global Carbon Project (GCP).

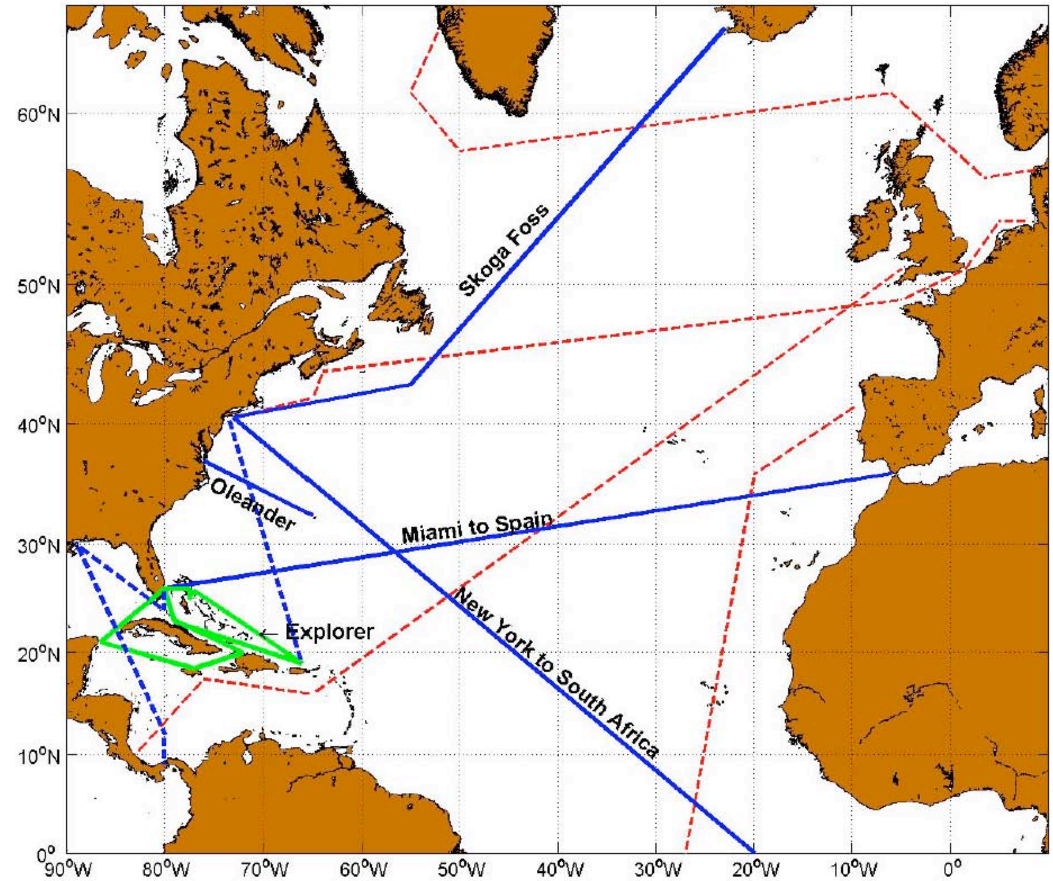

Figure 9. VOS pCO_2 lines in the North Atlantic. The blue and green lines are those funded by COSP and are part of the GOOS XBT observing network. The dashed lines are the routes outfitted by our European partners as part of the proposed European Carbo-Oceans project.

Table 5. Operational milestones pCO_2 project

Fall 2003	Complete installation of pCO_2 system on Skogafoss (Iceland-Norfolk) line AX2
Spring 2004	Complete installation of pCO_2 system and TSG system on Columbus Waikato (Long Beach - New Zealand) line PX13
Summer 2004	Complete installation of pCO_2 system on Oleander (Bermuda-Norfolk)
Winter 2004/2005	Complete standardized data reduction and quality control scheme for all ships Start submitted data to LDEO on routine basis for contextual QC
Spring 2005	Complete installation of pCO_2 system on Sealand Express (Iceland-Norfolk)
Fall 2005	Complete installation of pCO_2 system on 24°N line (Miami-Gibraltar)
Winter 2005/2006	Install system on VOS ship in North Pacific
Spring 2006	Install system on NOAA survey ships in Gulf of Mexico (Gunther) and Bering Sea (Rainer)

Data for all projects will be distributed to the community at large through a Live Access Server within two years after collecting the data.

At a national level the CO_2 COSP effort is part of the US Carbon Cycle Science Plan. Its critical role in the overall US ocean science effort is outlined in the multi-agency implementation plan, the Ocean Carbon and Climate Change plan (Doney, 2004). Information about the programs linked to, or which are a part of, COSP-CO_2 can be found in Table 6.

Table 6. Web sites of the CO_2/COSP program and program partners

Data sites for pCO_2 data from ships:	
AOML	http://www.aoml.noaa.gov/ocd/gcc
PMEL	http://www.pmel.noaa.gov/uwpco2/
LDEO	http://www.ldeo.columbia.edu/res/pi/CO2/
Program sites:	
CLIVAR	Climate Variability and Predictability: www.clivar.org
SOLAS	Surface-Ocean Lower Atmosphere Study: www.uea.ac.uk/env/solas/
IOCCP	International Ocean Carbon Coordination Project: www.ioc.unesco.org/ioccp
IGBP	International Geosphere-Biosphere Project: www.igbp.kva.se/cgi-bin/php/frameset.php
IMBER	Integrated Marine Biogeochemistry and Ecosystem Research: http://www.igbp.kva.se/cgibin/php/
WCRP	World Climate Research Program: www.wmo.ch/web/wcrp/wcrp-home.html
GCP	Global Carbon Project: http://www.globalcarbonproject.org/

Key References

Bender, M., S. Doney, R. A. Feely, I. Y. Fung, N. Gruber, D. E. Harrison, R. Keeling, J. K. Moore, J. Sarmiento, E. Sarachik, B. Stephens, T. Takahashi, P. P. Tans, and R. Wanninkhof, A Large Scale Carbon Observing Plan: *In situ* Oceans and Atmosphere (LSCOP), pp. 201, Nat. Tech. Information Services, Springfield, 2002.

Feely, R. A., J. Boutin, C. E. Cosca, Y. Dandonneau, J. Etcheto, H. Y. Inoue, M. Ishii, C. Le Quere, D. Mackey, M. McPhaden, N. Metzl, A. Poisson, and R. Wanninkhof, Seasonal and interannual variability of CO_2 in the Equatorial Pacific, *Deep Sea Research II*, *49*, 2443-2469, 2002.

Doney, S., The Ocean Carbon and Climate Change Report, UCAR, Boulder, 2004.

Houghton, J. T., Y. Ding, D. J. Griggs, M. Noguer, P. J.v.d. Linden, and D. Xiaosu, Climate Change 2001: The Scientific Basis: Contribution of Working Group I to the Third Assessment Report of the Intergovernmental Panel on Climate Change (IPCC), pp. 944, Cambridge University Press, Cambridge, England, 2001.

Sabine, C. L., M. Heimann, P. Artaxo, D, C. E. Bakker, C. - T. A. Chen, C. B. Field, N. Gruber, C. Le Quéré, R. G. Prinn, J. E. Richey, P. R. Lankao, J. A. Sathaye, and R. Valentini, Current Status and Past Trends of the Global Carbon Cycle*, Scope*, in press, 2003.

Sabine, C. L., R. A. Feely, N. Gruber, R. Key, K. Lee, J. L. Bullister, R.Wanninkhof, C. S. Wong, D. W. R. Wallace, B. Tilbrook, F. J. Millero, T. - H. Peng, A. Kozyr, T. Ono, and A. F. Rios, The oceanic sink for anthropogenic CO_2, *Science*, submitted, 2004.

Sarmiento, J. L., and N. Gruber, Sinks for anthropogenic carbon, *Physics Today*, *August*, 30-36, 2002.

Sarmiento, J. L., and S. C. Wofsy, A U.S. Carbon Cycle Plan, pp. 69, UCAR, Boulder, 1999.

Takahashi, T., S. G. Sutherland, C. Sweeney, A. P. Poisson, N. Metzl, B. Tilbrook, N. R. Bates, R. Wanninkhof, R. A. Feely, C. L. Sabine, J. Olafsson, and Y. Nojjiri, Global sea-air CO_2 flux based on climatological surface ocean pCO_2, and seasonal biological and temperature effects, *Deep-Sea Research II*, *49*, 1601-1622, 2002.

Takahashi, T., S. C. Sutherland, R. A. Feely, and C. E. Cosca, Decadal variation of surface water pCO_2 in the Western and Central Equatorial Pacific, *Science*, *302*, 852-856, 2003.

2.3 IN SITU DATA REQUIREMENTS FOR RECENT SITU SEA SURFACE TEMPERATURE ANALYSES

by Richard W. Reynolds, National Climatic Data Center, Asheville, North Carolina

Sea surface temperatures (SST) are an important indicator of the state of the earth's climate system as well as a key variable in the coupling between the atmosphere and the ocean. Accurate knowledge of SST is essential for climate monitoring, prediction and research. It is also a key surface boundary condition for numerical weather prediction and for other atmospheric simulations using atmospheric general circulation models. SST is also important in gas exchange between the ocean and atmosphere, including the air-sea fluxes of carbon.

The longest data set of SST observations is based on observations made from ships. These observations include measurements of SST alone as well as temperature profiles with depth. However, the observations of SST alone dominate the data sets and account for more than 90% of the observations. These observations are typically made by measuring the temperature in buckets of seawater collected from the ship or by the ship engine intake temperature gauge. Typical RMS errors from ships are larger than 1°C and may have daytime biases of a few tenths of a degree C (Kent et al., 1999). Although the earliest observations were taken in the first half of the 19th century, sufficient observations to produce a global SST analysis were not available until about 1870.

SST observations from drifting and moored buoys began to be plentiful in the late 1970s. These observations are typically made by thermistor or hull contact sensor and usually relayed in real-time by satellites. Biases in the SSTs from buoys can occur in some designs. For example, significant diurnal heating of the hull may occur under low wind conditions with some hull configurations. Although the accuracy of the buoy SSTs varies, it is usually better than 0.5°C, which is better than ship SSTs. In addition, typical depths of the observations are roughly 0.5 m rather than the 1 m and deeper depths from ships.

In late 1981, accurate SST retrievals became available from the Advanced Very High Resolution Radiometer (AVHRR) instrument, which has been carried on many NOAA polar orbiting satellites. These retrievals improved the data coverage over that from *in situ* observations alone. The satellite retrievals allowed better resolution of small-scale features such as Gulf Stream eddies. In addition, especially in the Southern Hemisphere, SSTs could now be observed on a regular basis in many locations. Because the AVHRR cannot retrieve SSTs in cloud-covered regions, the most important problem in retrieving SST is to eliminate clouds. The cloud clearing algorithms are different during the day and the night because the AVHRR visible channels can only be used during the day. After clouds have been eliminated, the SST algorithm is derived to minimize the effects of atmospheric water vapor. The satellite SST retrieval algorithms are "tuned" by regression against quality-controlled buoy data (McClain et al., 1985). This procedure converts the satellite measurement of the "skin" SST (roughly a micron in depth) to a buoy "bulk" SST (roughly 0.5 m).

Future improvements in the SST observing system will primarily be due to new satellite data. In roughly the last decade, new infrared sensors, such as the Moderate Resolution Imaging Spectroradiometer (MODIS), have become available on other satellites. Beginning in December 1997, SSTs began to be available on the Tropical Rainfall Measuring Mission (TRMM) satellite. Additional microwave instruments have become available in late 2002 and more are planned. SSTs from microwave instruments have lower spatial resolution than from IR instruments.

However, microwave instruments are able to retrieve SSTs in cloud-covered regions where IR instruments cannot.

The purpose of this discussion is to examine the accuracy of climate scale SST analyses, which are defined at spatial scales of 1^{o} and larger and temporal scales of one week and longer. It is necessary to briefly review the types of errors that can be expected. With any measurements, the first type of error is random error, which is the observational error caused by the instrument and/or the observer. Most analyses attempt to account for the random errors. For analyses with non-uniform data distribution, the second type of error is sampling error. The sampling error usually becomes important in an analysis and may become more important than the random error. Analyses such as the optimal interpolation (OI) compute the combined random and sampling analysis error. However, these combined analysis errors are only estimates because they depend on estimates of the data and analysis error covariances in space and time. The remaining source of error is bias error, which is due to a systematic difference between one instrument or a set of instruments and another.

For the examination of errors, the OI analysis (Reynolds and Smith, 1994 and Reynolds et al., 2002) was used. At each analysis grid point, the OI objectively determines a series of weights for each observation. The OI method assumes that the data do not contain long-term biases. Because satellite biases occur, an optional step using a Poisson's Equation can be carried out to remove satellite biases relative to *in situ* data prior to the OI analysis. This method adjusts any large-scale satellite biases and gradients relative to the *in situ* data. In the OI procedure, various error statistics are assigned that are functions of latitude and longitude. The OI has been computed since November 1981 and uses *in situ* and AVHRR satellite data.

It is useful to examine the input data for one week. Figure 1 shows the input data from the AVHRR and the *in situ* data along with the completed OI analysis. The result clearly shows that the satellite coverage is far superior to the *in situ* coverage. The missing satellite data here is due to cloud cover, which restricts the retrievals. Microwave data would have better coverage since microwave retrievals can be in cloudy regions unless it is raining. Because of the high density of satellite observations, the sampling and random errors are relatively small and are usually below 0.3^{o}C on monthly scales on a 5^{o} grid. However, satellite bias errors can be large even on monthly scales. Reynolds (1993) found that the absolute satellite biases from the AVHRR instrument exceeded 2^{o}C during the eruptions of Mt. Pinatubo. Biases on these scales lasted several months, and biases greater than 0.5°C persisted for almost a year. In addition, biases may occur at the end of a satellite instrument's useful lifetime and can also reach levels of 2^{o}C. Reynolds et al. (2004) showed an example for the AVHRR instrument on the NOAA-14 satellite. The aerosol biases are often confined to the tropics. However, biases due to instrumental problems can occur at higher latitudes. As it is not known when biases of this magnitude will occur, the *in situ* network must be designed to correct the potential bias to the required accuracy.

Before examining the *in situ* network, it is necessary to define an acceptable bias error. A maximum allowed bias error was specified by Needler et al. (1999) for a 500 km by 500 km box on a weekly time scale as 0.2-0.5^{o}C. Because satellite biases do not change greatly from weekly to monthly periods and because a 5^{o} latitude-longitude box is close to a 500 km box (only 10% larger at the equator), the minimal bias accuracy considered here will be less that 0.5^{o}C on a monthly 5^{o} grid. This modification was made for computational convenience and to simplify buoy deployment plans.

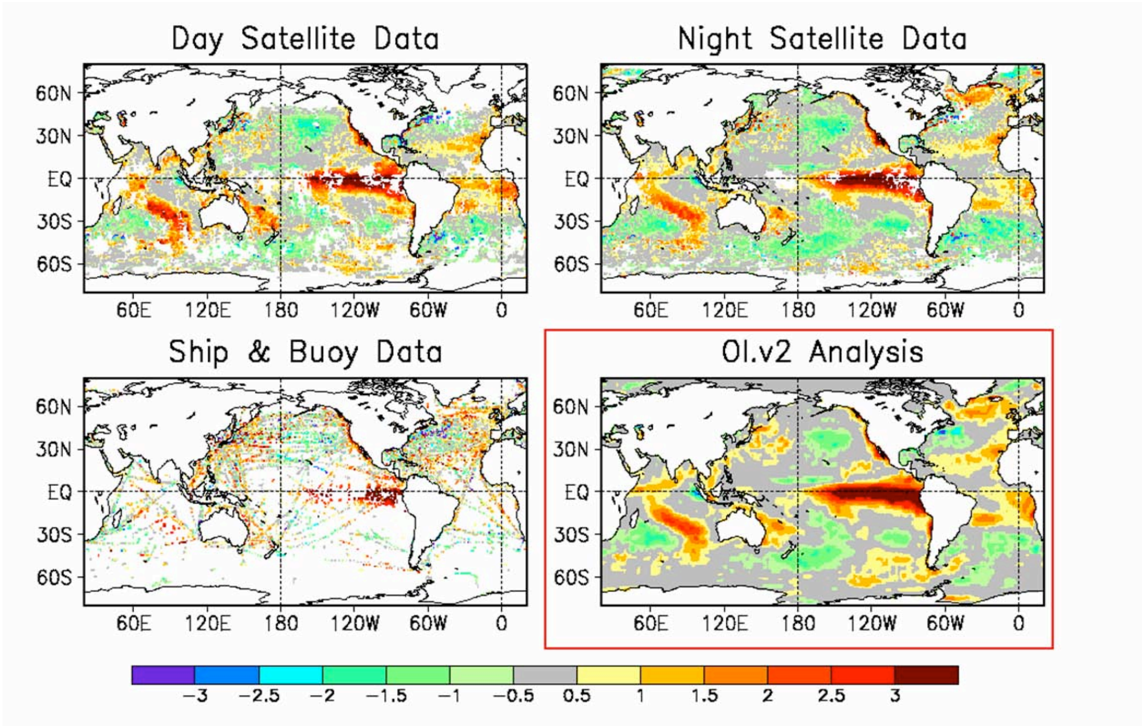

Figure 1. Weekly SST input data for the optimum interpolation (OI) SST analysis for December 14-20, 1997. The top two panels show the daytime and nighttime AVHRR satellite SST data. The bottom left panel shows the *in situ* (ship and buoy) SST data. The analysis (bottom right panel) combines the satellite and *in situ* data into a smoothed product. The data and analyses are shown as anomalies (departures from normal) in °C. White regions indicate missing data. Please note the superior coverage of the satellite data compared to the *in situ* data.

To better design an *in situ* network to correct satellite SST biases, it was necessary to examine the scales of the bias. Zhang et al. (2004a) examined the biases and extracted the six most important bias fields. The next step is to compute the buoy density needed to reduce any potential satellite bias errors below 0.5°C over the global ocean. Because there is no systematic way to define the bias errors, the OI analysis was used with simulated satellite and *in situ* data. Satellite data were simulated by each of the six spatial bias patterns at the locations of the actual satellite data. Buoy data were simulated without bias error on regular grids at various grid resolutions. By design, the simulated satellite biases will be reduced by the simulated buoy data. The purpose is to determine the buoy grid density at which the satellite SST biases can be reduced to within the required accuracy (i.e., below 0.5°C) over the global ocean. The spatial satellite biases are scaled to give a potential satellite bias error of 2°C if there were no buoy data. The word 'potential' is used in the definition as a reminder that the satellite bias was scaled.

The results of the simulations are described in detail in Zhang et al. (2004b). The simulations show that at least 2 buoys are needed on a 10° grid to reduce the potential satellite bias below 0.5°C. To use this requirement in actual distributions, it is necessary to determine how to combine ship and buoy data in the results. Because ship observations are noisier (random error of 1.3°C, Reynolds and Smith 1994) than buoy observations (random error of 0.5°C), roughly 7 ship observations are required to have the same accuracy of one buoy observation. Therefore, an equivalent-buoy-density (*EBD*) is defined as: $\boldsymbol{EBD = n_b + n_s/7}$. Here $\boldsymbol{n_b}$ and $\boldsymbol{n_s}$ are the number of buoys and number of ships in a 10° box, respectively.

The *EBD* was defined for each month, and then averaged seasonally for operational buoy deployment. An example is shown in Figure 2 for October – December 2003. Boxes poleward of 60°N and 60°S were not shown along with boxes with less than 50% ocean by area as well as boxes in Hudson Bay and the Mediterranean Sea. Color shading is used in the figure to help indicate where additional buoys are needed, as indicated in the figure caption. The number of additionally needed buoys to reach *EBD*=2 for all shaded boxes in Figure 2 has been computed. The number of buoys needed in the middle latitude Southern Hemisphere (60°S-20°S) shows a rapid drop with time in the mid 1990s due to the increase in the number of buoys deployed (Reynolds et al. 2002). For the three-month average shown in Figure 2, 189 additional buoys are needed between 60°N-60°S, of which 102 are needed between 60°S-20°S, 65 between 20°S-20°N, and 22 between 20°N-60°N.

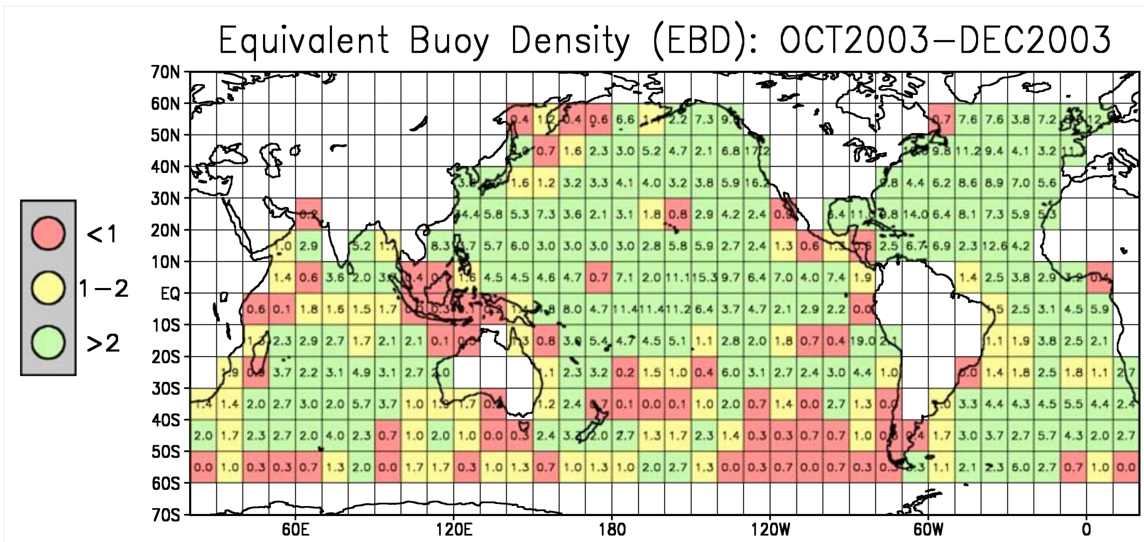

Figure 2. Equivalent buoy density (*EBD*) with respect to a 10° grid for the season of October – December 2003. Green shading is used where *EBD*≥2 and indicates regions where no more buoys are needed. Red shading is used where *EBD*<1 and indicates regions which have a high priority to be filled with more buoys. Yellow shading indicates where1≤*EBD*<2 and indicates regions where more buoys are needed but at a lower priority than the red shading.

The current *in situ* observation network was designed for other purposes and is thus not necessarily the most efficient network for climate SST. For example, the *EBD* exceeds 5 in most of the North Atlantic Ocean (see Figure 2), while the *EBD* is less than 2 in a large number of boxes in the Southern Oceans. For climate purposes alone, the current buoy distribution could be relocated in some regions, especially in the North Atlantic and North Pacific. These results have already had an influence on future buoy deployments. The NOAA Atlantic Oceanographic and Meteorological Laboratory (AOML) is now using figures like Figure 2 to guide surface drifting buoy deployments. It is hoped that this study will be useful in helping to objectively define requirements for an integrated ocean observing system.

References

Kent, E. C., P. G. Challenor and P. K. Taylor, A statistical determination of the random observational errors present in voluntary observing ships meteorological reports, *Journal of Atmospheric & Oceanic Technology*, *16*, 905-914, 1999.

McClain, E. P., W. G. Pichel, and C. C. Walton, Comparative performance of AVHRR-based multichannel sea surface temperatures, *Journal of Geophysical Research*, *90*, 11587-11601, 1985.

Reynolds, R. W., Impact of Mount Pinatubo aerosols on satellite-derived sea surface temperatures, *Journal of Climate*, *6*, 768-774, 1993.

Reynolds, R. W. and T. M. Smith, Improved global sea surface temperature analyses using optimum interpolation, *Journal of Climate*, *7*, 929-948, 1994.

Reynolds, R. W., N. A. Rayner, T. M. Smith, D. C. Stokes and W. Wang, An improved *in situ* and satellite SST analysis for climate, *Journal of Climate*, *15*, 1609-1625, 2002.

Reynolds, R.W., C. L. Gentemann, and F. Wentz, Impact of TRMM SSTs on a climate-scale SST analysis, *Journal of Climate*, *17*, in press, 2004.

Zhang, H.-M., R. W. Reynolds, and T. M. Smith, Bias characteristics in the AVHRR sea surface temperature, *Geophysical Research Letters*, *31*, L01307, doi:10.1029/2003GL018804, 2004a.

Zhang, H.-M., R. W. Reynolds, and T. M. Smith, Evaluation of recent SST *in situ* observing system for climate, Draft paper, to be submitted to the Journal of Climate, 2004b.

2.4 SURFACE CURRENTS TO IDENTIFY SIGNIFICANT PATTERNS OF CLIMATE VARIABILITY

by Peter Niiler[1] and Nikolai Maximenko[2]

[1]Scripps Institution of Oceanography, La Jolla, California
[2]International Pacific Research Center, Honolulu, Hawaii

The oceans affect the changes of the habitability of the globe because they are the earth's principal time-varying reservoirs of thermal energy and moisture. If the temperature of the air over the oceans departs from SST, there is an exchange of heat and moisture, and the temperature of the air, because of its low heat capacity, adjusts to SST. The thermal energy reservoirs of the ocean depend crucially upon the ocean circulation patterns. The climate change of the atmosphere is best understood and modeled if the general circulation of the oceans and its changes are well known.

Climate scientists use global ocean circulation models to study and predict the processes that cause climate change. If models replicate the recent, short-term climate changes it is thought that they can also be used to predict longer time scale changes into the future. The accuracy of global climate change models can only be determined with spatially and temporally extensive data sets on the currently evolving state of the circulation and property distributions of the global oceans. Global surface velocity data is important for the description and modeling of the modes of climate change because surface currents are one of the principal physical causes for the changes of SST.

The global ocean surface currents and SST are measured with satellite located drifting buoys in an international program called the "Global Drifter Program". This program began in 1988 and since 1992 there have been about 625 drifters in the ocean. In late 2003, the number of drifters has increased to about 950 and in 2004 a full deployment of 1250 drifters will be implemented. These data have been combined with satellite altimeter data to make the 1992-2004 time mean atlas of ocean currents at 15m-depth over the entire globe. Both the geostrophic and wind driven currents have been computed. Before climate related changes of the surface circulation are computed, a time mean must be defined, which has been the first task in the 2003-04 period.

Figure 1 displays the absolute sea level computed from drifter and satellite altimeter data (Niiler *et al.,* 2003); the geostrophic component of the near surface current is computed from the gradient of this sea level distribution just like air currents are computed from sea level pressure maps. The wind driven, or Ekman, current is shown in Figure 2. Ekman currents are calculated using Ralph and Niiler (1999) parameterization with coefficients optimized to recent data of the pair of satellites called GRACE (Gravity Recovery And Climate Experiment), and are to the right of the wind in the northern hemisphere and to the left of the wind in the southern hemisphere. These digital ocean surface current data are available on request from: pniiler@ucsd.edu. The raw data and the research publications that have used these data to understand ocean circulation are available from: http://www.aoml.noaa.gov/phod/dac/dacdata.html/.

To observe the climate variability of ocean currents, the short-term variability has to be 'averaged' out. Statistical measures can be established to show how well any map of surface current represents a phenomenon described on specified space and time scales. Drifters sample the ocean currents accurately, but not very often. Satellite altimeter data can be used to compute

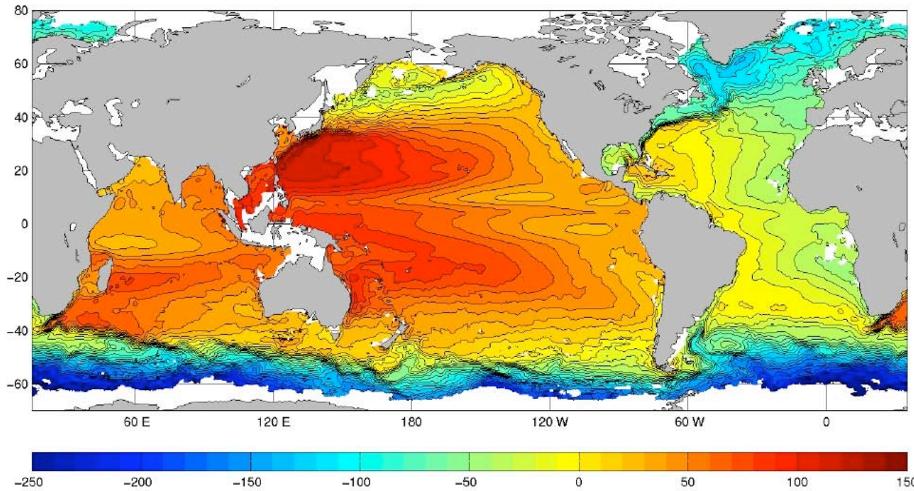

Figure 1. 1992-2002 absolute mean sea level computed as described by Niiler et al., 2003 but with Ekman parameterization optimized to the GRACE data. Contour interval is 10 cm.

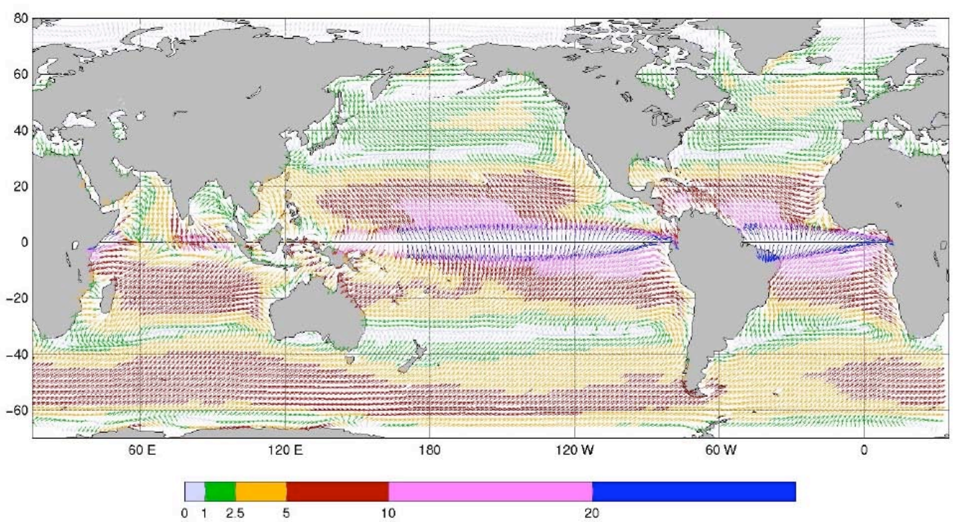

Figure 2. 1992-2002 mean Ekman currents at 15 m depth as calculated using NCAR/NCEP re-analysis winds and Ralph and Niiler (1999) parameterization optimized to the GRACE data. Colors of velocity vectors correspond to their magnitudes (colorbar is in cm/s).

geostrophic ocean currents on a regular time interval, but since ocean currents contain significant Ekman components and are not in geostrophic balance near the equator, their derivations from altimeters also use drifter observations. A combined field of circulation derived from drifters and altimeters (and wind) will have less sampling bias and is more accurate than the fields derived separately. The following performance measures are established for obtaining confidence intervals for surface circulation:

Table 1. "Surface Velocity Program (SVP)" Statistical confidence measures

FISCAL YEAR	2002	2003	2004	2005	2006	2007	2008
1) Observe the mean circulation confidence on a 0.5ºx0.5º spatial scale							
	30%	35%	50%	55%	65%	75%	85%
2) Observe the 50 km spatial scale mesoscale eddy energy* confidence							
	60%	65%	70%	75%	80%	85%	operational
3) Compute maps of seasonally varying tropical current systems with confidence							
	50%	60%	70%	70%	75%	75%	operational
4) Interannual, large spatial scale (2º Lat. x 5º Long.) current systems with confidence							
	30%	35%	40%	45%	50%	50%	

* Eddy energy can also have seasonal and interannual variability.

References

Niiler, P. P., N. A. Maximenko, and J. C. McWilliams, Dynamically balanced absolute sea level of the global ocean derived from near-surface velocity observations, *Geophysical Research Letters*, *30(22),* 2164, doi:1029/2003GL018628, 2003.

Ralph, E. A., and P. P. Niiler, Wind driven currents in the Tropical Pacific, *Journal of Physical Oceanography*, *29*, 2121-2129, 1999.

2.5. SEA SURFACE PRESSURE

Excerpt from The Second Report on the Adequacy of the Global Observing Systems for Climate in Support of the UNFCCC, April 2003, with contributions by
Ed Harrison, Pacific Marine Environmental Laboratory, Seattle, Washington

Parameter: Surface air pressure

Main climate application

Surface air pressure data provide vital information about atmospheric circulation patterns in the climate system. Long-term air pressure data compilations can be used to assess changes, fluctuations and extremes in climatic circulation regimes. Such analyses aid ongoing efforts to assess the relative importance of anthropogenic and natural influences, and to estimate possible future impacts of atmospheric circulation changes on human activities.

Contributing baseline GCOS observations

The GCOS surface network (GSN), is a subset of approximately 1000 stations that supports the global network of locations that provide local and regional-scale observations. The GSN promotes best practice and is a baseline against which to assess the long-term homogeneity of the rest of the surface network. The GSN must be augmented with additional surface air pressure data, especially over the oceans, in order to provide more detailed patterns of spatial changes, fluctuations and extremes in atmospheric circulation.

Other contributing observations

There is a Surface Synoptic (SYNOP) pressure network of 7000 surface recording stations as well as additional national and research observing networks. Voluntary Observing Ships, fixed platforms, moored and drifting buoys often report air pressure over the ocean.

Significant data management issues

GSN data management is achieved by a combination of national data management organizations, GCOS GSN monitoring and analysis centers, and CBS GCOS lead centers.

Analysis products

Time series are created for individual stations, station differences, regional averages, hemispheric averages, and global averages. Gridded fields are created via objective analysis and data synthesis (e.g., reanalysis, HadSLP). Indices of climatic phenomena (e.g., Southern Oscillation, North Atlantic Oscillation), means, seasonal cycles, and extreme events can all be derived from surface air pressure observations.

Current capability

Gridded global monthly, seasonal and annual surface air pressure compilations are capable of resolving important information about circulation changes and fluctuations over the last 120-150 years. Examinations of circulation extremes and storminess require daily surface air pressure data. To date, this has mainly been temporally limited to the last half-century or less and also spatially limited to parts of the Northern Hemisphere, especially in the US-European sector.

Issues and priorities

The following issues and priorities exist:

- Data archaeology, digitization of longest available data records
- Access to daily data
- Homogenization of daily data as much as possible

- International surface air pressure database
- Testing climate model data sets against observational data products
- Checking on reduction to standard gravity

Conclusions (contributed by Ed Harrison)

Surface pressure variability drives a direct oceanic response that can be a significant source of sampling troubles in some situations, or the sea level/surface pressure link. Surface pressure is highly important as an indicator of the strength of the atmospheric circulation, and is important to know over the ocean even without wind stress.

Because 1 mb of sea level pressure (SLP) uncertainty translates directly into 1 cm uncertainty in sea level height (assuming an inverse-barometer relationship), we would like to have the local point instantaneous error in SLP analysis from the operational meteorological centers be 0.5 mb or less. This is a challenging standard. At the moment, in places where there is little *in situ* error, we have root mean square (RMS) differences (between the European Centre for Medium-Range Weather Forecasts (ECMWF) and the National Center for Environmental Prediction (NCEP)) of as much as 2-3 mb or point errors up to about three times this value. Typical maximum point errors presently over the better-sampled parts of the globe *may* be in the 2-3 mb range. If we enhance the global drifter array by attaching sensors to measure SLP, it is believed to be possible to decrease the maximum point uncertainty to 1 mb or better. This is the present goal. To further improve, better SLP sensors will also be needed on ships.

2.6 AIR-SEA EXCHANGE OF HEAT, FRESH WATER, MOMENTUM

by Robert C. Weller, Woods Hole Oceanographic Institution, Woods Hole, Massachusetts

Goal: to identify changes in forcing functions driving ocean conditions and atmospheric conditions

The ocean has a distinct role in governing the variability of the earth's atmosphere, land, and ocean. It carries heat poleward from the equatorial regions where the sun shines most strongly. It releases heat and moisture into the lower atmosphere to drive weather patterns, storms and hurricanes, and longer period climate variability that includes the El Niño-Southern Oscillation. The ocean, which covers 70% of the earth, can store 1100 times more heat than the atmosphere due to the larger heat capacity and density of water. The upper 2.5 m of the ocean, when warmed 1°C, thus stores an amount of heat that would raise the entire column of air above it 1°C as well. As a consequence, an anomalously warm region of the ocean has the potential of releasing considerable energy to the atmosphere above and thus driving the weather on short time scales and, if the release of heat persists, can alter climate. Energy to drive the atmosphere is also transferred from the ocean by evaporation, and the ocean's role as a source of moisture is also critical to understanding weather and climate as well as the global cycle of freshwater. The ocean also stores 97% of the earth's water and plays a major role in the global cycle of freshwater that heavily impacts agriculture and human activities; 86% of the evaporation and 78% of the precipitation occur over the ocean. The third exchange of interest is that of momentum, in other words, determining how the surface winds drive the ocean currents and how the ocean surface provides drag to the atmosphere. The shallow, wind-driven ocean currents are of particular interest because of their role in transporting the surface waters that are warmed and cooled by exchanges with the atmosphere.

One goal of the NOAA Climate Observation Program is to collect long, accurate time series of the air-sea exchanges of heat, freshwater, and momentum at key locations around the world's ocean, aiming toward 16 such sites by 2006 and building to 51 of these sites, known as ocean reference stations. A second goal is to use these accurate observations together with surface meteorological and air-sea flux observations from Volunteer Observing Ships (VOS) to produce daily maps of the air-sea fluxes over the global ocean.

What are the reasons for these goals? First, these maps will show where and how much heat and freshwater are exchanged between the ocean and atmosphere, show how the winds drive the surface currents, and thus quantify the exchanges between the ocean and atmosphere that play important roles in weather, climate, and the global water cycle. Thus, we would be able to document, for example, the impact on climate of years of anomalous heat and freshwater loss to the atmosphere by a region of the ocean and to search for connections across the globe between rainfall anomalies on land and where and how much freshwater was released from the ocean. At present, due to sparse observations and large uncertainties in the present estimates of the air-sea exchanges, we cannot (across time scales that range from hurricanes to decadal) determine across the globe whether or not anomalous ocean conditions cause or result from anomalous atmospheric conditions. We look to new, accurate flux maps with good temporal and spatial resolution to show where and when change in the ocean leads or lags change in the atmosphere.

Second, the flux maps will provide the surface forcing for numerical ocean models now used to investigate oceanic variability and the ocean's role in climate; such models are now forced using climatological surface fluxes or other fields of fluxes that have large uncertainties, which in turn add uncertainty to the results of the ocean modeling. The ocean, as pointed out above, has a large ability to store heat. It also has a three-dimensional circulation that is much slower than that of the atmosphere, with the deep waters being exposed to the atmosphere only every 100 years or so. Accurate surface forcing is needed as we look to improve the ability of these ocean models to properly simulate the mixing, overturning, and decadal and longer term transport, storage, and release back to the atmosphere of heat and freshwater.

Third, atmospheric models are now forced at the sea surface with sea surface temperature fields and use their own parameterizations to develop surface fluxes of heat, fresh water, and momentum. By comparison with data from the ocean reference stations that are being deployed by the NOAA Climate Observation Program, the air-sea fluxes in these atmospheric models are found often to have large differences from the actual fluxes. This needs to be addressed because many ocean modelers use the atmospheric model flux fields as their surface forcing and also because the role of the ocean in weather and climate variability in these atmospheric models and in climate models that use the same or similar code may not be well represented. Moreover, accurate fields of the surface exchanges are required for evaluation of the ability of coupled ocean-atmosphere climate models, such as those used in IPCC (Intergovernmental Panel on Climate Change) predictions of future climate change, to simulate present day climate. Such evaluations are necessary if we are to have confidence in the future climate change scenarios predicted by these models.

Fourth, surface flux fields are widely used in observational studies by the oceanographic research community studying large scale ocean circulation and its impact on climate, in synthesis with sub-surface measurements, to determine the transports of water and heat across basin scale ocean sections. In particular, the fields of momentum flux are required to determine the wind-driven or Ekman component of the ocean transport, and the fields of heat, fresh water, and momentum flux are needed to provide surface forcing conditions for analyses of hydrographic (ocean temperature and salinity) data which use inverse techniques to estimate the transports of water with different, characteristic temperatures and salinities.

Finally, the accurate time series from the ocean reference stations serve several key functions: 1) provide accurate long time series of known accuracy at key locations which are of high value as records of variability and change in the coupling of the ocean and atmosphere, 2) help to calibrate and validate remote sensing, 3) provide the ability to examine the realism of the air-sea fluxes in numerical weather and climate models, 4) provide accurate records of the surface forcing to be used in studies of oceanic response to and interaction with the atmosphere, and 5) provide critical points across the ocean basins to use as standards and anchor sites to develop the global air-sea flux fields through the synthesis of data from the diverse sources needed to achieve daily, global fields.

The context for this element of the Climate Observation Program can be illustrated by Figure 1, which compares time series of air-sea fluxes from a surface mooring of the type being deployed at the Ocean Reference Stations. Monthly means of wind stress (momentum flux) and net heat flux from two state of the art numerical weather models, one from the National Center for Environmental Prediction (NCEP) and one from the European Centre for Medium Range Weather Forecasts (ECMWF) are plotted against the monthly means from the buoy and monthly means from flux fields developed at Southampton Oceanography Centre (SOC) from VOS observations. Note not only how large the differences in net heat flux are between the NCEP and ECMWF monthly means and those of the buoy but also that the NCEP heat fluxes have the wrong sign during June and July. Indeed the ECMWF model indicates through the year about 50 W m^{-2} less heat into the ocean than observed, and the NCEP has a negative bias of about 100 W m^{-2}. Errors of this size have been seen at other sites. Yet, recent ongoing efforts to understand the dynamics of the upper ocean and the ocean's role in climate, such as the World Ocean

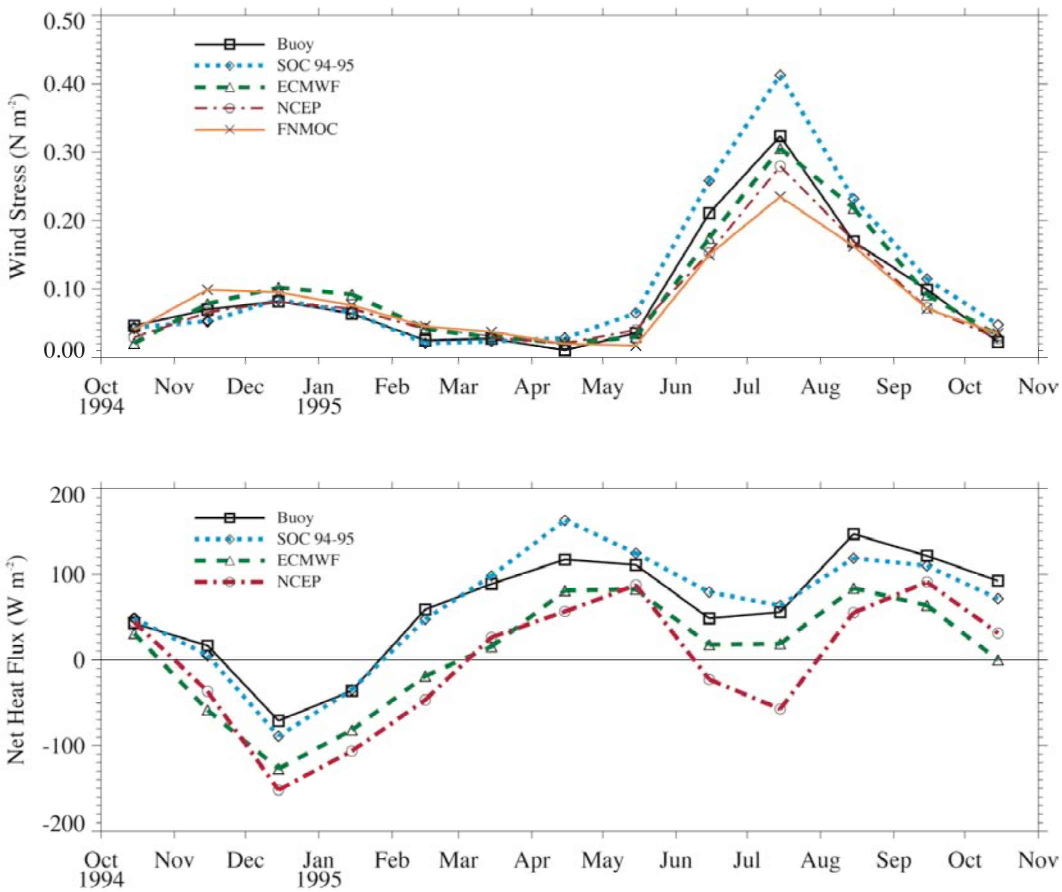

Figure 1. Monthly mean wind stress (momentum exchange) (upper) and net heat flux (positive into the ocean) at a mooring deployed in the northern Arabian Sea for one year.

Circulation Experiment (WOCE), the Tropical Ocean-Global Atmosphere Program (TOGA), and the Climate Variability (CLIVAR) Program have identified the need for monthly mean net heat flux estimates to be available with accuracy of better than 10 W m^{-2}. Consistent accuracy targets for precipitation and wind stress are 0.01 mm hr^{-1} and .01 N m^{-2}, respectively. These lead to target accuracies for sea and air temperature of 0.1°C, for wind speed of better than 5%, for relative humidity of better than 3%, for incoming shortwave of better than 10 W m^{-2}, and for incoming longwave of better than 5 W m^{-2}. Some of the errors cancel, and these target accuracies typically allow the 10 W m^{-2} goal in the net heat flux to be met at present. A more challenging objective for the future of this effort motivated by the desire to better understand long term climate change would be to resolve mean values of the net heat flux well enough to be able to sense shifts in the surface radiation budget associated with changes in greenhouse gases and aerosols, thus requiring the reduction of errors in the net heat flux to approximately 4 W m^{-2}.

This element of the Climate Observation Program is in its initial phase. The goals are to deploy and maintain the Ocean Reference Stations and, using these time series as the critical accurate reference observations, to produce global maps of the air-sea fluxes of heat, freshwater, and momentum. The challenge is a significant one, requiring cruises to deploy and maintain each Ocean Reference Station once per year, requiring dedicated on the land and at sea calibration efforts to obtain the sought after accuracies in these unattended surface moorings, and also requiring well-instrumented VOS that cross the ocean basins to obtain essential complementary information about the spatial variability in the surface meteorological and air-sea fluxes and in the differences between these observed fields and the model and remotely-sensed fields used to synthesize global maps.

At present, one Ocean Reference Station is operating under the stratus clouds off the coast of northern Chile (20°S, 85°W) and one in the tropical western North Atlantic (15°N, 51°W). Immediate plans are to add a third Ocean Reference Station north of Hawaii and to complement the sensors on four existing TAO-TRITON sites in the equatorial Pacific to qualify them as Ocean Reference Stations. A pilot project has been conducted, using past buoy, model, and satellite data, to test and develop the methodology of producing air-sea fluxes fields on basin scales. Figure 2 shows a comparison of the long-term (1988 to 1997) mean sum of the latent and sensible heat flux components from a new flux product developed by L. Yu at Woods Hole Oceanographic Institution (WHOI) with the SOC climatology and mean fields from ECMWF and NCEP. The WHOI product produced by data assimilation methodology compared the best against the buoy data available from this period; this pilot project affirmed the approach being taken.

As yet, the observations made under this component are sparse. The data are withheld and not used in preparation of model fields by the operational weather and climate modeling centers. This is done so that the Ocean Reference Station time series can serve as an independent assessment of model performance and thus to stimulate the ongoing dialog that will motivate improvements to these models. The sparse Ocean Reference Stations are building evidence of biases and errors in the models at the few sites now occupied. A milestone for the project will be when the deployed buoys cover many of the critical weather and climate regimes of the global ocean and thus can be used to identify and fix problems in these models common to all sites as well as to identify issues unique to specific regimes.

With sufficient funding and with new observatory technology to be developed under the Ocean Observatory Initiative of the National Science Foundation, the deployment of the planned numbers of Ocean Reference Stations is entirely feasible. Each site will require a regular, once per year commitment of ship time and of on land and at sea calibration. Significant milestones will be achieved when the Ocean Reference Stations in each basin provide time series from the meteorological and air-sea regimes characteristic of those basins. When that is accomplished, the time series from these moorings will provide compelling evidence to drive the process of partnering with the atmospheric modeling community to improve the realism of those models and to produce basin scale flux fields of the desired accuracy. These time series sites should be accompanied by accurate measurements from the ship that deploy and recover the mooring to provide in-the-field calibration of the moored time series. They should also be accompanied by improved measurements from selected VOS to obtain direct observations of the spatial variability of the surface meteorological and air-sea flux fields. Practical considerations require the implementation of a hierarchy of VOS observations systems. The state of the art instrumentation of two to three long cross-basin ship lines (with preference for the high resolution XBTs lines) in each ocean basin will provide estimates of high absolute accuracy. A few hundred ships recruited under the VOSClim program will have improved instrumentation and sufficient documentation to allow any measurement biases to be quantified and corrected through comparison with the Ocean Reference Stations. The majority of the international VOS fleet (some six thousand ships) will continue to provide basic observations over large areas of the world oceans which must be verified against the higher quality observations from the specially chosen ships and buoys. These observing efforts should be accompanied by quality control efforts, by close interaction with the

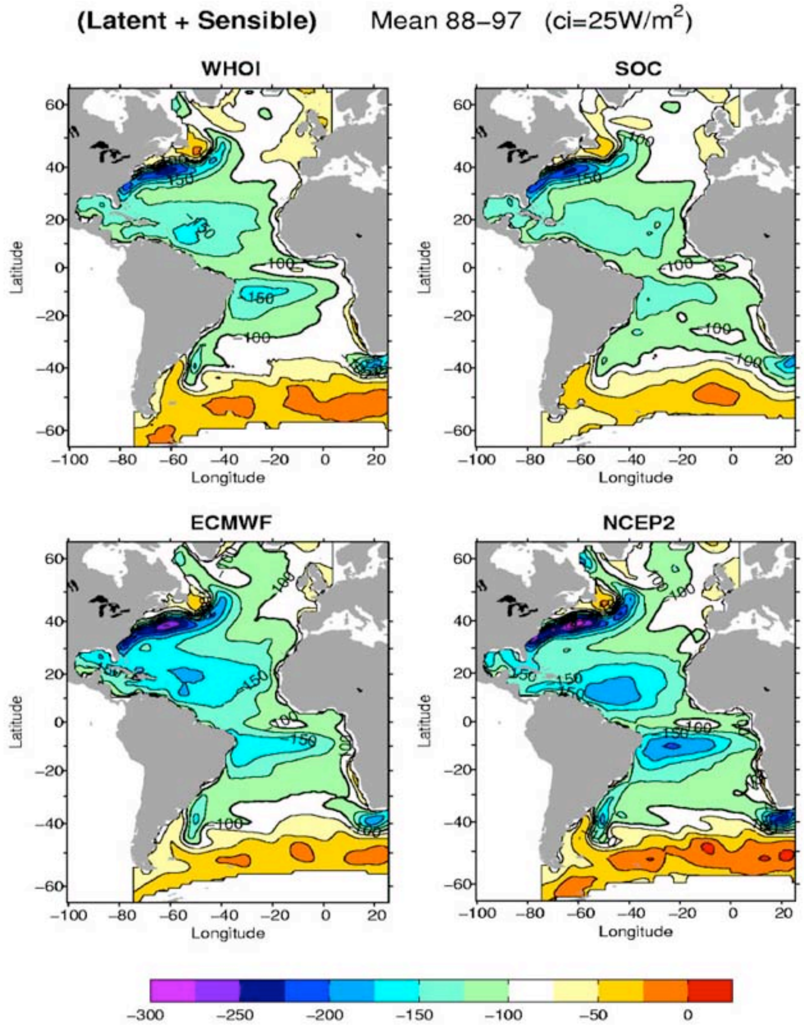

Figure 2. Four maps of the long-term (1988-1997) sum of latent and sensible heat flux components in the Atlantic basin. WHOI was produced by L. Yu at WHOI and validated against buoy data. SOC is a climatological product based on VOS data; ECMWF and NCEP2 are analyses based on those numerical weather prediction models.

atmospheric modeling centers and those working up remotely-sensed fields at the ocean surface, and by production of global fields of the air-sea exchanges of heat, freshwater, and momentum that are made available to the research and operational communities.

Acknowledgement:
This section on air-sea exchange of heat, fresh water and momentum was written with input from Drs. Peter Taylor and Simon Josey of the Southampton Oceanography Centre, UK, Dr. Chris Fairall of the NOAA Environmental Technology Laboratory, Boulder, Colorado, and Dr. Frank Bradley of the Commonwealth Scientific and Industrial Research Organization (CSIRO), Canberra, Australia.

2.7 OCEAN HEAT AND FRESH WATER CONTENT AND TRANSPORTS

by Lynne Talley, Scripps Institution of Oceanography, La Jolla, California

2.7.1 Introduction

Heat and freshwater transport changes as well as changes in local air-sea exchange are recorded in variations in ocean temperature and salinity distributions. Here, the state of ocean temperature and salinity distributions in the year 2003 is compared with longer-term means. To the extent that heat and freshwater transports have been computed and compared with historical estimates, these results are reviewed. Changes in air-sea fluxes are considered in section 2.6. A calculation of heat and freshwater transports is included based on atmospheric conditions in 2003, to be compared with the long-term mean values of these transports. Global anomalies of SST and surface salinity are shown in Section 2.7.2.

The ocean is then divided into regions based roughly on the primary circulation and processes affecting these regions. Section 2.7.3 summarizes heat content changes through 2003 in the upper ocean, including the ENSO condition in the tropical Pacific, variations in the tropical Atlantic and Indian Oceans, and Pacific Decadal Oscillation and North Atlantic Oscillation variations in the Pacific and Atlantic.

Section 2.7.4 summarizes temperature, salinity and transport variations in waters affected strongly by the global thermohaline circulation. These regions include the Arctic and Nordic Seas, the subpolar North Atlantic, the intermediate and deep water layers of the subtropical and tropical Atlantic, and NADW layers farther downstream from the North Atlantic. Variations in deep and bottom waters formed in the Antarctic are also described.

In section 2.7.5, bulk estimates of heat and freshwater transports for 2003 are reviewed. In section 2.7.6, papers published in 2003 that report changes in ocean temperature and salinity structure, mostly for data collected prior to 2003 compared with longer-term averages, are summarized.

2.7.2 Global upper ocean temperature and salinity

Sea surface temperatures for 2003, from the NOAA CDC website, are displayed in Fig. 2.7.1, showing the annual mean temperature and the monthly anomalies from the long-term means (Reynolds et al., 2002).

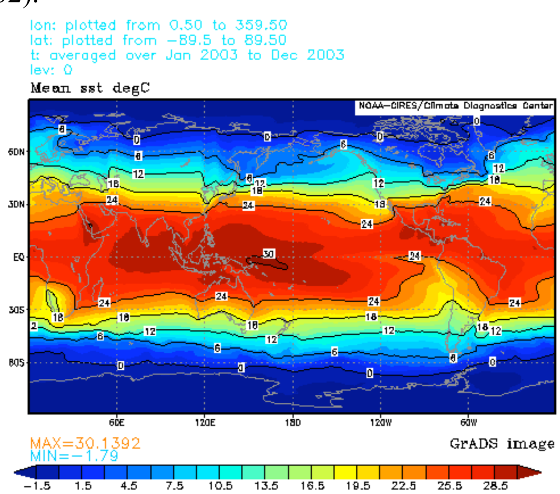

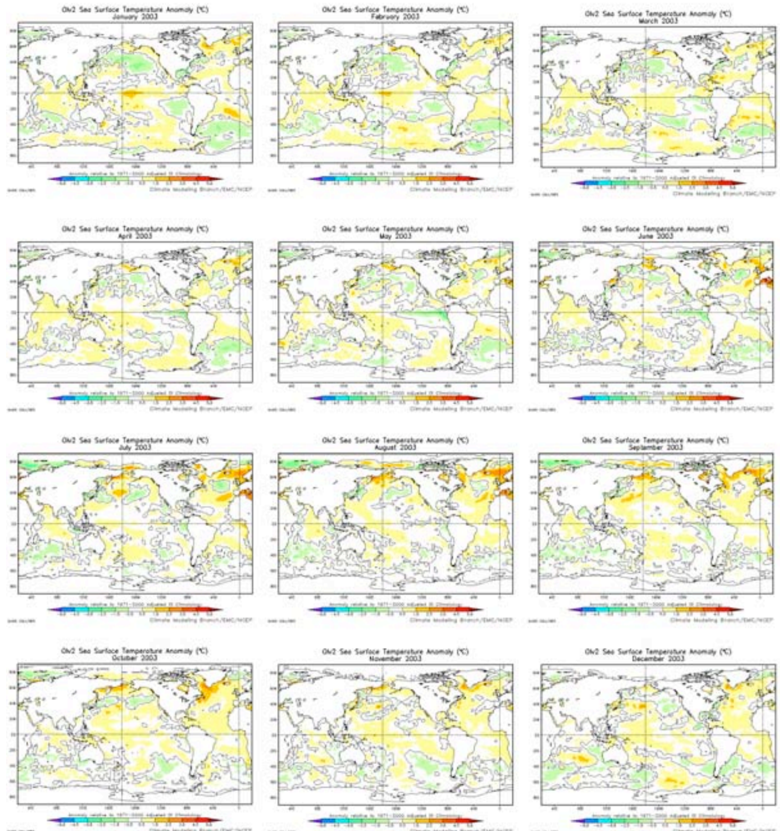

Figure 2.7.1. (a) Annual mean sea surface temperature, 2003. Image from the NOAA-CIRES Climate Diagnostics Center, Boulder, Colorado, (http://www.cdc.noaa.gov/). (b) 2003 monthly SST anomalies from the 1971-2000 mean (Reynolds et al., 2002). Images from NCEP (2004): http://www.emc.ncep.noaa.gov/research/cmb/sst_analysis/.

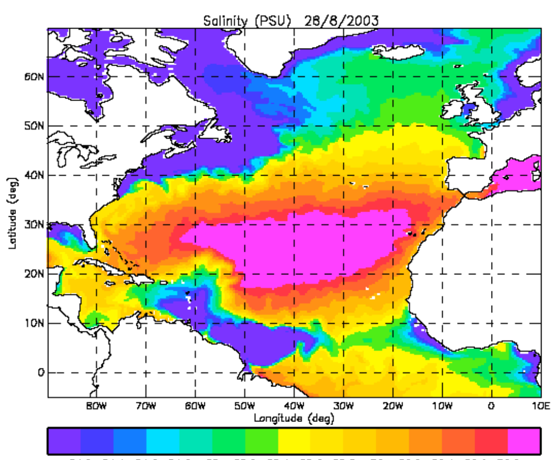

Figure 2.7.2. Surface salinity analysis from U.K. operational assimilating model. Maps are provided of temperature and salinity down to 300 m, incorporating ARGO and XBT data. **(**http://www.met-office.gov.uk/research/ocean/operational/foam/realtime/index.htm)

2.7.2.1 Global upper ocean temperature and heat content in 2003 (XBT and ARGO)
The ARGO float program has begun monitoring subsurface temperature and salinity in many regions. The ARGO float deployment at the beginning and end of 2003 (Fig. 2.7.3) shows the quick ramping up of this program. Operational products of subsurface temperature and salinity fields and anomalies for comparison with long-term means are not yet available. In upcoming years, these will likely be routinely reported.

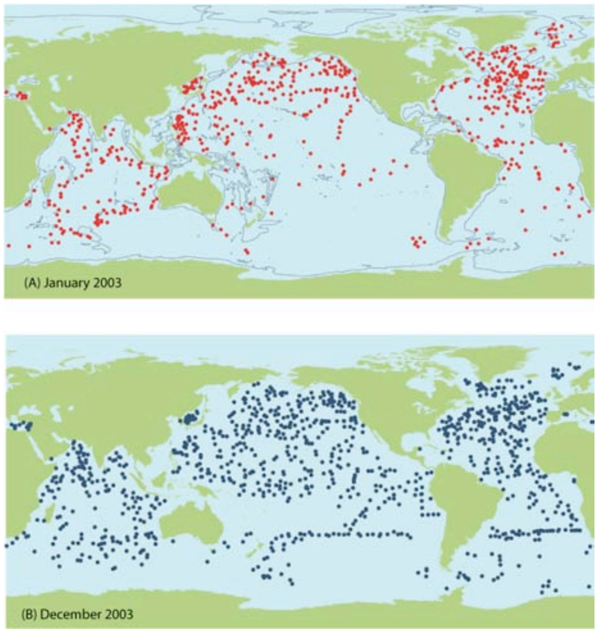

Figure 2.7.3. ARGO floats in January 2003 and in December 2003. (http://w3.jcommops.org)

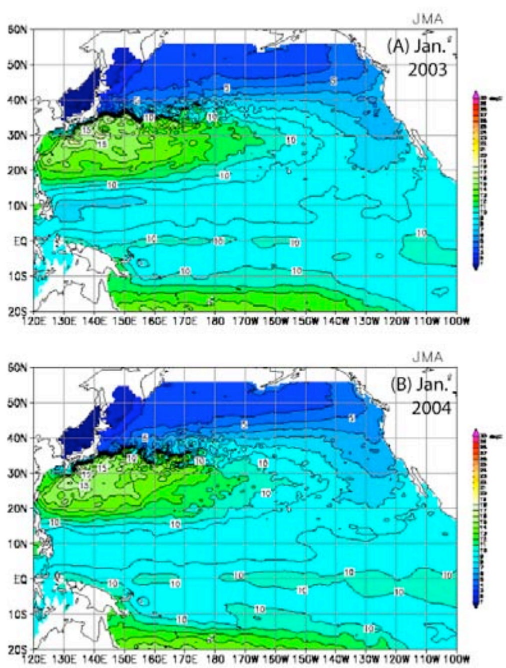

Figure 2.7.4. Examples of monthly sub-surface temperature analysis (available from surface down to 400 m), for (a) January 2003 and (b) January 2004, at 400 m, from the Japan Meteorological Agency, incorporating ARGO and XBT data, http://argo.kishou.go.jp/index.html)

2.7.2.2 Global upper ocean salinity in 2003 (ARGO and hydrographic observations)
Global coverage of salinity is expanding with ARGO. At this point, only preliminary analyses are publicly available. Because of the impact of salinity changes on decadal and longer climate variability, and because of the use of salinity as a signature of such climate variability, it is imperative that regular salinity products be compiled and made publicly available as soon as possible. To be most useful, both the observed and anomaly fields should be shown. A fast turnaround taxes the ability to calibrate salinity observations in near real-time, and so products with some lag time would clearly be desirable. An example of products currently available from IFREMER is shown in Figure 2.7.5.

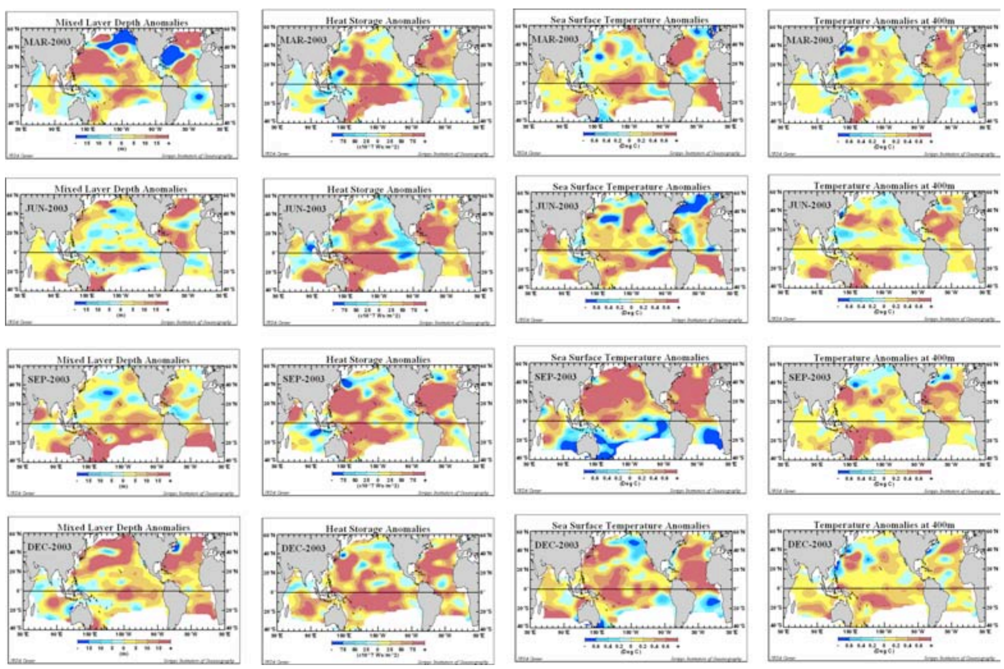

Figure 2.7.5. Year 2003 anomalies of (a) mixed layer depth, (b) heat storage, (c) surface temperature and (d) 400 m temperature based on subsurface temperature data, from the Joint Environmental Data Analysis Center (JEDAC) at Scripps Institution of Oceanography (http://jedac.ucsd.edu).

Variations in North Atlantic sub-surface salinity in recent years have been reported by Dickson et al. (2003) and Curry et al. (2003). These changes are hailed as harbingers of variations associated with the North Atlantic intermediate/deep overturn, and are discussed in section 2.7.4.

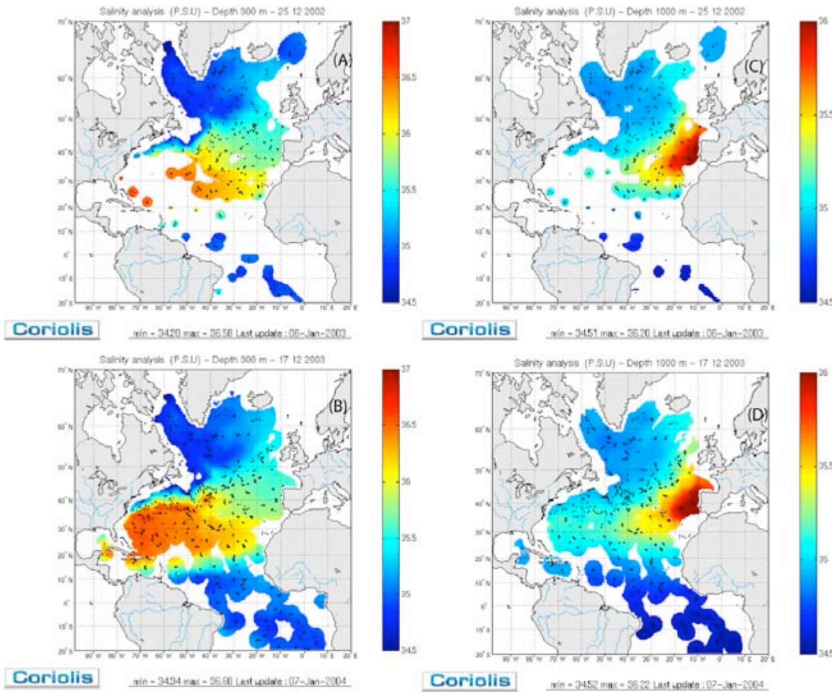

Figure 2.7.6. Example of salinity analyses from the Coriolis project (IFREMER, Brest, France), based primarily on ARGO data. (a) December, 2002, (b) December 2003, at 300 m, (c) December 2002, and (d) December 2003 at 1000 m, showing increase in data coverage. (http://www.coriolis.eu.org/coriolis/cdc/atlantic_area.htm)

2.7.3. Basin-wide upper ocean variations

Upper ocean variations in temperature, salinity and circulation are strongly associated with the natural modes of variability, variously identified as El Nino Southern Oscillation (ENSO) (2.7.3.1), the Pacific Decadal Oscillation (PDO) (2.7.3.2), the tropical Atlantic dipole, the Indian dipole (both in 2.7.3.3), the Southern Annular Mode (SAM) (including the Antarctic Circumpolar Wave or Antarctic Dipole Mode) (2.7.3.4), and the North Atlantic Oscillation (NAO) and Arctic Oscillation (AO) (or Northern Annular Mode) (2.7.3.5). The state of these modes and the ocean response in 2003 to the modes is reviewed in this section. It is hoped that this introduction to ocean responses in 2003 will spur compilation of more operational products that display these responses. Examples shown were accessed online.

2.7.3.1 Heat content variations and ENSO (from McPhaden, 2004)

El Niño Southern Oscillation (ENSO) variability is intimately linked to alternating stages of oceanic heat content build-up and discharge from equatorial latitudes. These heat content variations are mediated by wind-forced equatorial waves and affect sea surface temperature (SST) through equatorial upwelling and other processes. Changes in SST then feedback to the atmosphere to modify surface wind and precipitation patterns. The slow seasonal evolution of upper ocean heat content and its feedbacks to the atmosphere account for the characteristic interannual time scale of ENSO. The predictability of ENSO likewise derives from the deterministic wind-driven ocean dynamics that govern this slowly evolving upper ocean thermal field.

According to the "recharge" oscillator theory for ENSO: 1) a build-up of excess heat content along the equator is a prerequisite for the occurrence of El Niño; 2) the equatorial Pacific is purged of excess heat content during El Niño; and 3) the time between El Niños is determined in part by the time it takes to recharge equatorial latitudes with excess heat once again. Empirically it has also been determined that the magnitude of El Niño SST anomalies usually scales in proportion to the magnitude of the prior heat content build-up.

Zonally integrated heat content along the equator provides a convenient index for interpreting ENSO variability in terms of recharge oscillator theory. One definition of heat content for this purpose is the integrated warm water volume (WWV) above the 20°C isotherm between 5°N–5°S from the eastern to the western boundary of the Pacific. It is evident from the WWV time series and the NINO3.4 SST index (see Figure 2.7.7) that a build-up in heat content along the equator has preceded all El Niños since 1980 by 2–3 seasons. The heat content build-up prior to the 2002–03 El Niño was about half that prior to 1997–98, and comparable to that prior to the 1986–87 and 1991–92 El Niños. Based on this heat content precursor, one would have expected maximum NINO3.4 SST anomalies for the 2002–03 El Niño to be significantly smaller than those in 1997–98 and similar to those in 1986–87 and 1991–92.

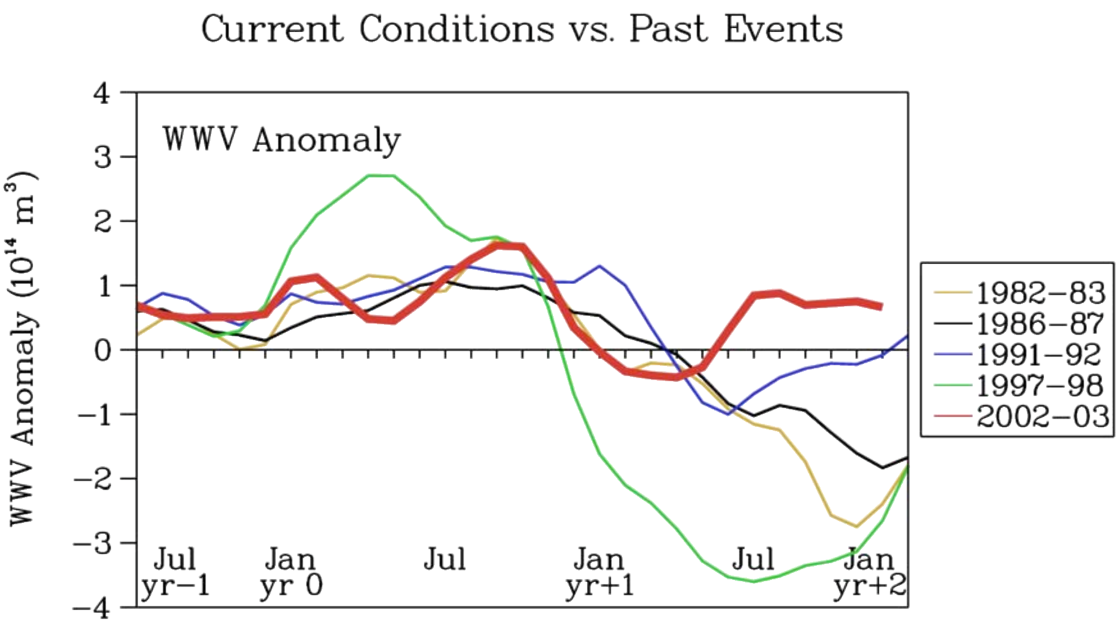

Figure 2.7.7. Monthly anomalies of warm water volume (5°N–5°S, 80°W–120°E above the 20°C isotherm) and NINO3.4 SST (5°N–5°S, 120°W–170°W) from January 1980 to December 2003. Warm water volume is based on a blended analysis of TAO/TRITON moored time series data and ships-of-opportunity expendable bathythermograph (XBT) data. Time series have been smoothed with a 5-month running mean filter for display.

WWV along the equator peaked in September 2002 after which it began to rapidly decrease, in accordance with the idea that El Niño should purge excess heat from the equatorial band. WWV became weakly negative in February–April 2003, consistent with the existence of a shallower than normal thermocline along the equator at that time. The steep plunge in WWV from September 2002 to February 2003 was a harbinger of the 2002-2003 El Niño's demise, though WWV subsequently rebounded to positive values in mid-2003 in response to renewed episodic westerly wind forcing (Figure 2.7.8). The persistence of this elevated WWV during the second half of 2003 is linked to slightly elevated El Niño-like SSTs in the equatorial Pacific that some forecast models indicate will persist into the Northern Hemisphere spring of 2004.

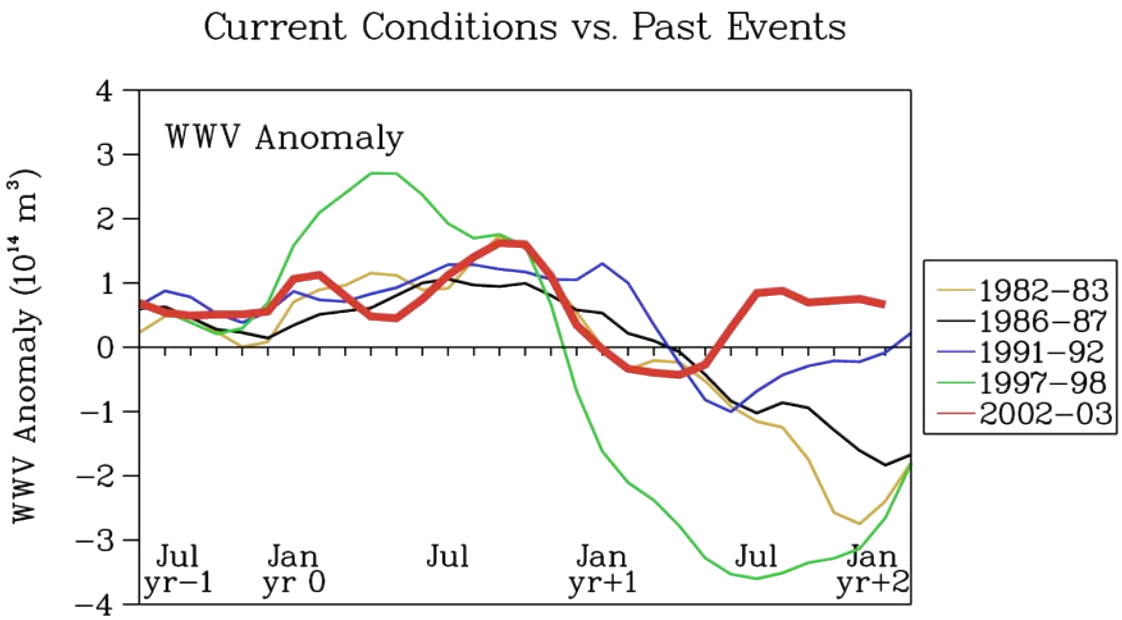

Figure 2.7.8. Monthly warm water volume (WWV) variations in the Pacific during El Niños since 1980, starting in July the year before each El Niño and ending in January the year after.

2.7.3.2. Upper ocean property variations in the mid-latitude Pacific and mid-latitude southern hemisphere

The extratropical Pacific and subtropical regions of the southern hemisphere respond to several identified climate modes. We examine the Pacific Decadal Oscillation here. The dominant Pacific mode is known as the Pacific Decadal Oscillation (PDO). It is meridionally symmetric about the equator. The Pacific Decadal Oscillation index shown in Fig. 2.7.9 is the leading eigenvector of the North Pacific SST (Zhang et al., 1997; Mantua et al., 1997). When the index is high, the tropical Pacific is warm and the high latitude Pacific is cold, and vice versa. A high PDO index is also associated with high pressure in the tropical Pacific and low pressure in the higher latitudes. The PDO spatial pattern is similar to that of ENSO, but without the very large peak in amplitude in the tropics. The PDO thus modulates the strength of ENSO; when the PDO index is high, ENSO is especially pronounced. The ocean and atmospheric changes in circulation, pressure, and temperature are well described although the governing dynamics are not well understood. Boundary regions bordering continents are especially impacted by PDO-variations in the ocean, with impacts on marine-based economics (fisheries) and coastal climate. When the PDO index is high, circulation in the Gulf of Alaska is stronger and less subpolar water enters the California Current. The Oyashio is also strong during high PDO.

The PDO was high in 2003, continuing from mid-2002. This followed a brief period of low PDO (1998-2002) preceded by a prolonged period of high PDO, which began in 1976. Because of its relatively long duration in any particular phase and because of the widespread ecological impacts of the phase of the PDO, much attention has been focused on identifying "regime shifts" such as that in 1976 as they happen, although a true shift can only be defined several (5 to 10) years after the fact.

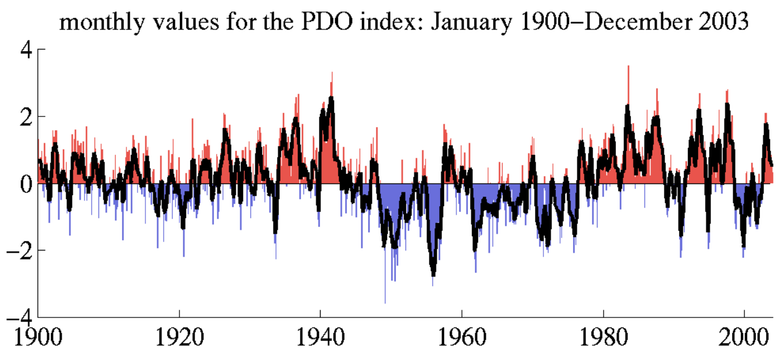

Figure 2.7.9. (a) Pacific Decadal Oscillation index (http://tao.atmos.washington.edu/pdo/).

SST anomalies in 2003 (Figure 2.7.1) were complicated, but generally showed the warm PDO phase, with warm eastern tropical waters and colder mid-latitude centers. This pattern is not as clear in Figure 2.7.5. The pattern also matches that of ENSO; the year 2003 included a weak ENSO (section 2.7.3.1).

2.7.3.3. Tropical Atlantic and Indian Oceans

The tropical regions of the Atlantic and Indian Ocean are influenced by upper ocean variations that might be separate from ENSO, although lagged ENSO response is also apparent. The tropical Atlantic experiences variability that has been described in terms of either a cross-equatorial dipole or as nearly independent modes north and south of the equator. There is no regularly produced index of a dipole or gradient mode. The Climate Diagnostics Center (CDC) and Climate Diagnostics Bulletin (CDB) report separate Tropical North Atlantic (TNA) and Tropical South Atlantic (TSA) mode indices (Figure 2.7.10). The CDB does not include an Indian Ocean SST index.

The tropical and mid-latitude Atlantic and the tropical Indian Ocean were anomalously warm throughout 2003 relative to a 1971-2000 climatology (Figure 2.7.1). The Atlantic warmth is reflected in positive values of the TNA and TSA throughout 2003 (Figure 2.7.10).

Regular sampling of the upper oceans is carried out using XBTs and ARGO floats. In each subtropical gyre there is also a zonal high density XBT section occupied approximately seasonally, with profiling to more than 800 m depth and close station spacing to produce the highest quality volume transport estimates. The South Atlantic section was begun in just 2002, so shown here is just one example of the section. (Figure 2.7.10b) As years of data accumulate, it will be possible to track interannual and then decadal variations in upper ocean temperature structure.

Indian Ocean variability has been described in terms of a dipole mode (Saji et al. 1999), although much of the Indian variability has also been described as heavily influenced by ENSO. There is no operational product or index describing this tropical variability. The southern Indian Ocean is affected by the Southern Annular Mode (section 2.7.3.4).

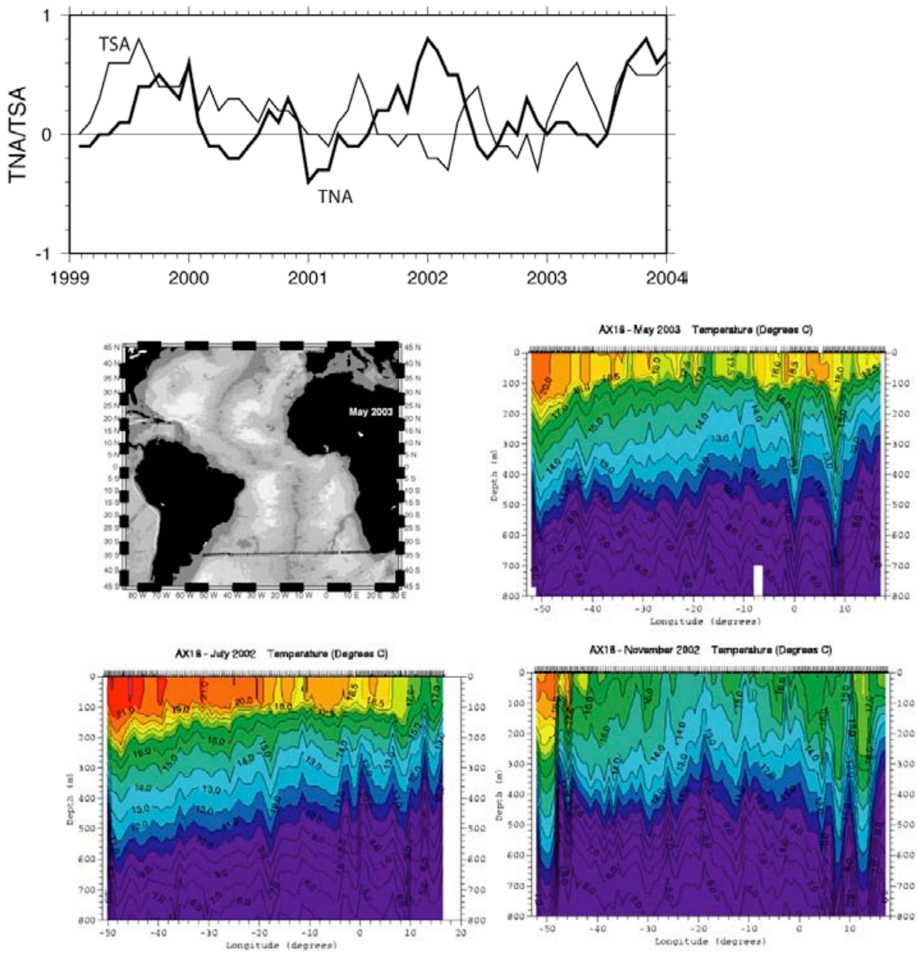

Figure 2.7.10. (a) Tropical North Atlantic (TNA) and Tropical South Atlantic (TSA) indices, including 2003. From the Climate Diagnostics Bulletin (http://www.cpc.noaa.gov/products/analysis_monitoring/CDB_archive.html). (b) Temperature from the first three occupations of the high density XBT section near 30°S in the South Atlantic (Garzoli, AOML, personal communication).

2.7.3.4. Southern Hemisphere Annular Mode

The Southern Hemisphere Annular Mode (SAM) or Antarctic Oscillation (AAO) is the major decadal mode of climate variation in the southern ocean (Thompson and Wallace, 2001). When the SAM index is high, the westerly winds are shifted to the south and are stronger; that is, the polar vortex is spun up. The associated Antarctic temperature changes are a colder interior of the continent and warmer region in the Antarctic Peninsula and ocean in the area of the Subantarctic Front. The AAO is tracked by the Climate Prediction Center (http://www.cpc.ncep.noaa.gov/products/precip/CWlink/daily_ao_index/aao/aao_index.html) (Figure 2.7.11).

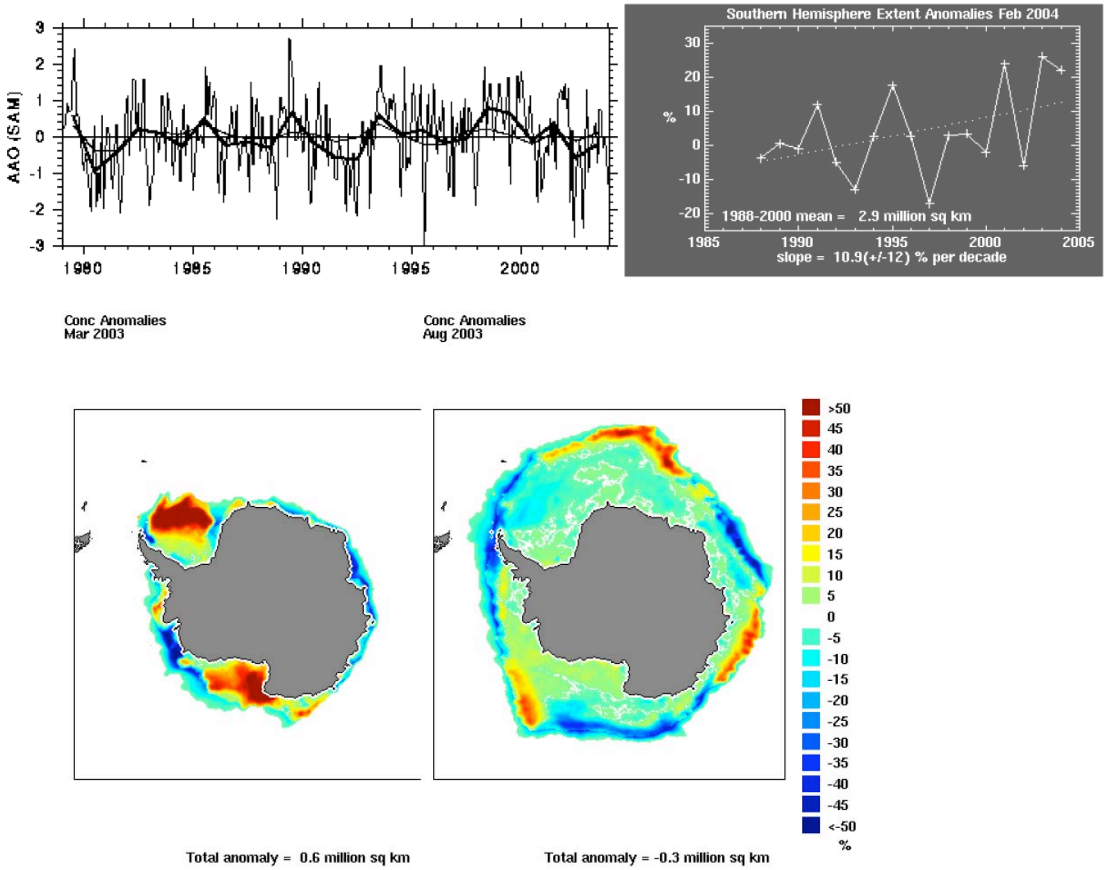

Figure 2.7.11. (a) AAO index based on monthly values from the Climate Prediction Center (thick: annual average; medium: JAS average; thin: monthly). (b) Sea ice index (Fetterer and Knowles, 2002). (c) and (d) Ice concentration anomaly in March and August 2003. (b, c and d from http://www.jpl.nasa.gov/pictures/seaice).

In 2003, the annual average AAO (SAM) was low, which would indicate a relatively warm Antarctic continent and cold subantarctic region of the ocean. The monthly SST maps (Fig. 2.7.1) show a strong dipole (wavenumber 2) pattern in zonal temperature in the first half of 2003, with warm regions south of Australia and in the eastern South Pacific, with cool regions in the central South Pacific and across the Atlantic, with an indication of eastward propagation. By winter (July), this pattern was breaking up. After the main winter months, the pattern was reversed with cold regions south of Australia and in the southeast Pacific. The monthly values of the AAO index are noisy, but reflect this shift, with positive values in mid-2003 shifting to negative values in late 2003. These negative values apparently dominate the annual mean. The AAO was clearly more negative in 2002, with the last period of persistently high AAO from 1997 to 1999.

In 2003, sea ice continued a long-term but very noisy upward trend around Antarctica. The patterns of sea ice concentration strongly reflected the zonal pattern of the SAM. An increase or decrease in sea ice extent has implications for the salinity of the surface layer and for salinity of dense waters formed on the shelves. See section 2.7.4.2 below for implications of changes in sea ice extent for dense water production.

2.7.3.5. North Atlantic Oscillation

The northern North Atlantic (subpolar region and adjacent Nordic Seas, including the Greenland, Iceland and Norwegian Seas) receives special attention because of its role in global overturning circulation and proximity of the affected surface currents to western Europe and the eastern U.S. The overturning culminating in deep and intermediate water formation in the Nordic and Labrador Seas is sometimes called the ocean "conveyor", and is global in extent. Considerable attention is paid to the strength and properties of this overturn, particularly in the North Atlantic where variations in salinity and temperature could presage variations in overturning strength. The magnitude of the effect of such circulation change on changes in SST, mid-latitude storm tracks, and continental climate is debated, but some level of climate change in response is probable.

A particular scenario that has received attention is the possibility of freshening of the surface layer of the northern North Atlantic, as a result of ice melt and/or changed precipitation patterns. Historically and in models, a freshened surface layer reduces or stops the convection that connects the surface to the intermediate layers in the Greenland and Labrador Seas. Freshwater from the Arctic impacts the Greenland Sea through the East Greenland Current, and impacts the Labrador Sea through Davis Strait as well as the East Greenland Current.

Northern North Atlantic climate change is strongly associated with the North Atlantic Oscillation (NAM) and its parent climate pattern, the Arctic Oscillation (AO) or Northern Annular Mode (NAM), which have quasi-decadal time scales. The NAO index measures the meridional atmospheric pressure gradient driving the westerlies. When the NAO index is high, the westerlies are in a northern position and strengthened, and vice versa.

The NAO index in 2003 was close to neutral, slightly on the high side, based on several available products (Figure 2.7.12).

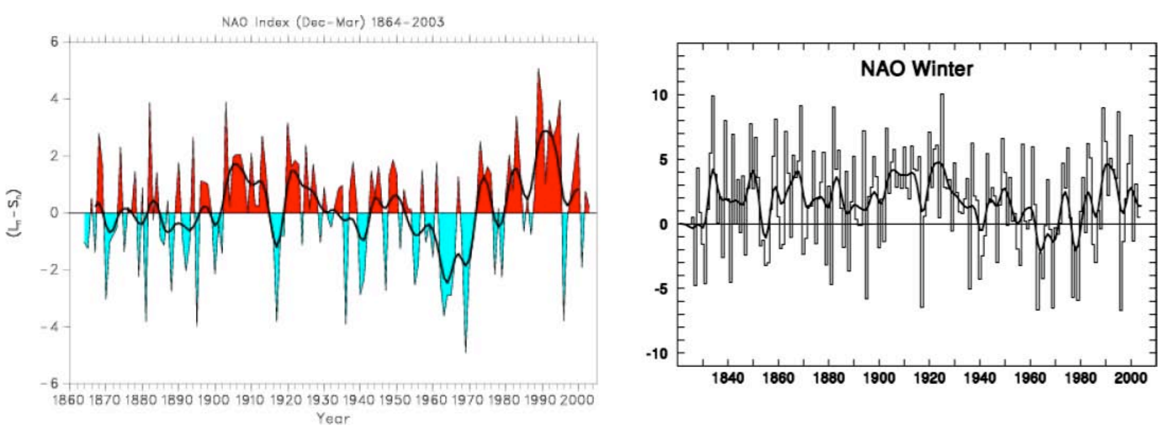

Figure 2.7.12. NAO index. (a) Winter Lisbon-Reykjavik SLP difference: image from http://www.cgd.ucar.edu/~jhurrell/nao.stat.winter.html (b) Gibraltar-Reykjavik pressure difference: image from http://www.cru.uea.ac.uk/cru/climon/data/nao/ (Climate Monitor Online, 2004).

Temperature anomalies along the zonal subtropical section crossing the North Atlantic at 24°N show an approximately 20-year signal (Fig. 2.7.13).

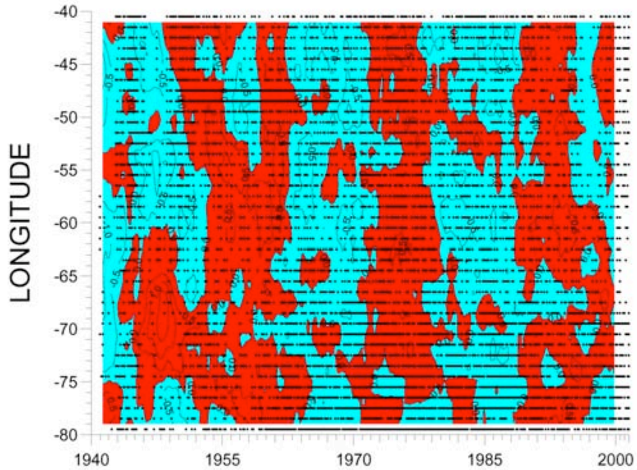

Figure 2.7.13. Surface temperature variations from BT and continuing XBT observations along 24°N showing an approximately decadal signal. Annual cycle and long-term trend were removed, and the data were filtered with a 3-year running mean (Baringer/AOML, personal communication).

2.7.4 Thermohaline (deep overturning) circulation

Deep overturn is affected by surface properties, particularly salinity and the presence and strength of a near-surface halocline. It is also affected by the overall stratification, hence properties, especially salinity, in and below the thermocline. A strong halocline supports surface cooling even to freezing without deep convection, whereas a weak halocline can permit deep overturn. Surface layer salinity is a function of regional precipitation and runoff and export of freshwater from winter ice-covered regions. Changes in freshwater content and sea ice extent thus have impacts on the thermohaline circulation, and are reviewed here.

The two sites that dominate thermohaline circulation of the global ocean are the deep and intermediate water formation sites in the northern North Atlantic, and at sites distributed around Antarctica. The waters from these two regions fill the global ocean, mixing with each other and with overlying thermocline waters. Upwelling occurs in many regions; this component of the thermohaline circulation is not yet well understood, but most likely involves a large amount of upwelling in the tropics and in the southern ocean. The North Pacific participates only weakly in thermohaline circulation because it is relatively fresh compared with the North Atlantic and Antarctic.

Major changes in thermohaline circulation are associated with glacial-interglacial changes in climate, with paleoclimate observations showing a weakening of the North Atlantic overturning and shift to shallower densities during the glacial periods. Variations in North Atlantic overturning are implicated in models of climate change, especially recent concepts of abrupt climate change (e.g. Alley et al., 2003). Southern Ocean overturning changes are the other end of the variability - models of thermohaline circulation variations often show alternating strength of overturn in the North Atlantic and Southern Ocean, with the implication that the present climate state is of strong North Atlantic overturn and relatively weak Southern Ocean overturn.

Changes in thermohaline circulation result from changes in the temperature/salinity distribution and less importantly from changes in air-sea flux. A saltier basin provides the greater and denser overturn. Changes in the circulation are a response to a buildup over many years, although the actual change is predicted to be quite sudden at some phases of the climate cycle.

There has been public discussion of the use of the phrase "thermohaline circulation" to describe the deep overturning circulation (Wunsch, 2002). Disagreement with this term arises from the actual forcing for the circulation, which is not primarily buoyancy-driven. We do not suggest that the phrase "thermohaline circulation" be dropped, since in fact the relative contrast in temperature and salinity between ocean basins is the determinant for the relative strength of deep overturn at the different sites.

2.7.4.1 North Atlantic overturn

The components of North Atlantic Deep Water sink from the surface at convection sites in the Nordic Seas, the Labrador Sea and the Mediterranean Sea. Within the North Atlantic and tropical Atlantic, these three source waters are readily distinguishable. Variations in their properties could be well defined by the completed ARGO network, and we anticipate that future summaries will draw effectively from this source (Figure 2.7.3). Current projects that regularly produce subsurface temperature maps do not include the deepest surfaces needed to characterize these water mass changes.

The source water for the sinking in the northern North Atlantic is upper ocean water that enters the North Atlantic from the southern hemisphere and from the Arctic. The Arctic source includes a fresh surface layer associated with continental runoff and the sea ice cycle. Major melting of Arctic sea ice was reported in 2002 and continued in 2003 (Figure 2.7.14). These fresh waters are exported to the North Atlantic in the East Greenland Current and through Davis Strait into the Labrador Sea. Freshening of upper ocean waters around the northern North Atlantic has been reported over the past several decades (Dickson et al., 2002, 2003 – their figures 2 and 4; Curry et al., 2003 - section 2.7.6 below). If continued, the freshening could initiate a weakening of the North Atlantic overturn.

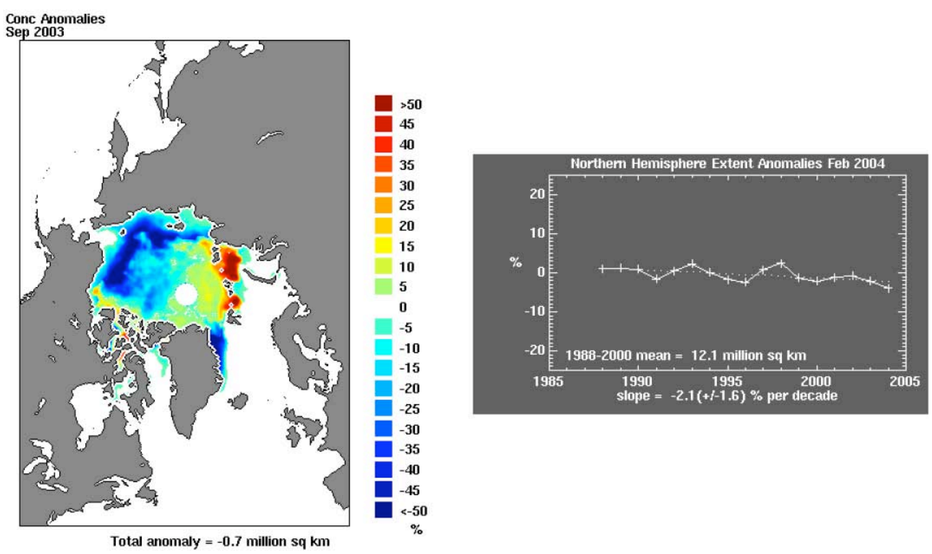

Figure 2.7.14. Arctic sea ice: (a) concentration in September 2003 and (b) multi-year time series of extent. (http://www.jpl.nasa.gov/pictures/seaice)

Time series of salinity from various locations around the northern North Atlantic shown by Dickson et al. (2002, 2003 – their Figure 4) show first the broad spatial scale of freshening and also the difficulty of interpreting a single year's observations. The important trends emerge only with several decades of data, and multi-year averaging.

The Deep Western Boundary Current (DWBC) in the subtropical North Atlantic carries the various component of the new North Atlantic Deep Water southward. As noted above, these include waters from the Labrador Sea at about 1500-2000 meters and from the Nordic Seas below this. Ongoing observations of the DWBC have shown the arrival of the extreme form of Labrador Sea Water that was formed in the1990s in the Labrador Sea (Molinari et al., 1998; Baringer, personal communication). As of 2002, continuing into 2003, freshening of the whole repeated section crossing the DWBC is apparent.

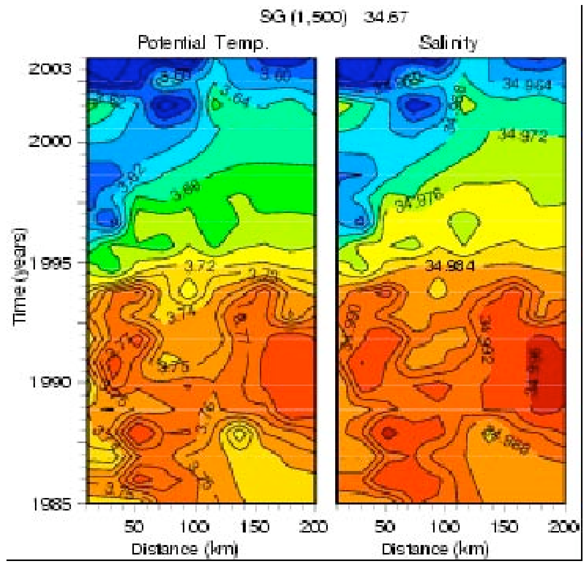

Figure 2.7.15. Hydrographic observations crossing the Deep Western Boundary Current east of Abaco at 26.5°N. Shown here are potential temperature and salinity at potential density σ_1= 34.67 (depth ~ 1500-1700 meters), showing the arrival of cold, fresh Labrador Sea Water after 1995. (from M. Baringer, NOAA/AOML)

2.7.4.2. Southern Ocean overturn

Bottom waters are formed around Antarctica through brine rejection in polynyas near the coast. Deep waters are formed by deep convection in the Weddell and Ross Seas. The global overturning circulation also has an important upward limb in the Circumpolar Current system located north of the winter ice edge northward through the Subantarctic Front, where deep waters, formed in the North Atlantic and modified in the deep Indian and deep Pacific Oceans, upwell.

Sea ice extent around Antarctica in 2003 was illustrated in section 2.7.3.4 and in Figure 2.7.11. The densest waters in the world are formed in polynyas in the coastal regions of Antarctica, over the continental shelves. With increasing sea ice production, as has been occurring in the Antarctic over the past several decades (noisy increase seen in Fig. 2.7.12b), denser shelf waters and hence denser bottom waters can be formed. With a decrease in summer ice melt (or smaller contrast between winter and summer ice extent), the freshwater surface layer inhibiting surface mixing would weaken, which also increases density and production of dense waters. Thus the changing sea ice conditions around Antarctica would appear to favor an increase in dense water production and density.

The southern ocean is also an important region of CO_2 exchange between the atmosphere and ocean; the highest column inventories of anthropogenic CO_2 in the global ocean are located in a circumpolar strip including the Subantarctic Front, and are most likely associated with the thick mixed layer north of the Subantarctic Front known as Subantarctic Mode Water. Fresh surface waters subducted north of this strip, concentrated in the southeast Pacific and southwest Atlantic, form the Antarctic Intermediate water, which is a major source of fresh water at mid-depth. Air-sea exchange of CO_2 is affected by upper ocean temperature. The role of the Southern Ocean overturn in inventories of atmospheric gases is illustrated in a 2003 publication of the global chlorofluorocarbon inventory (Figure 2.7.16a) based on WOCE (1990s) observations (Willey et al., 2004). Anthropogenic carbon content has been estimated from carbon observations and CFC observations (Figure 2.7.16b), and also shows a maximum in the circumpolar strip associated with Subantarctic Mode Water.

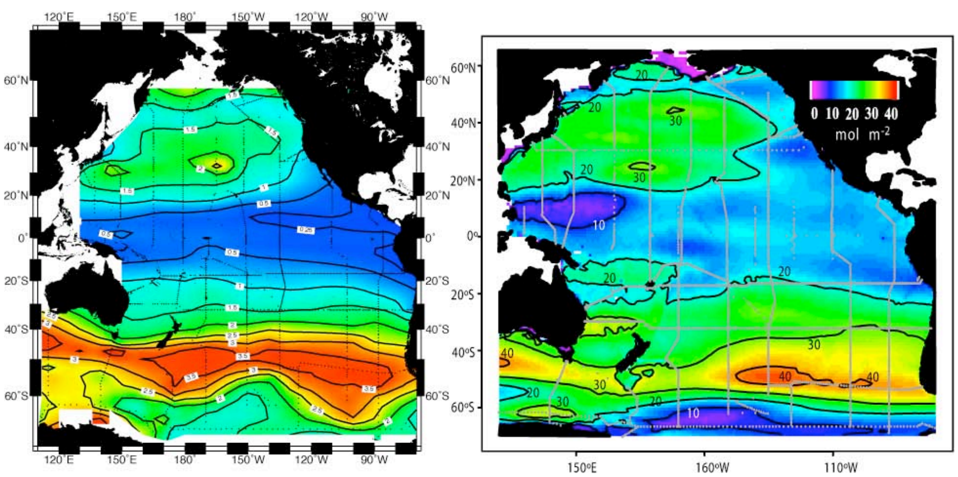

Figure 2.7.16. (a) Column inventory of chlorofluorocarbon (CFC-11), based on WOCE observations in the 1990s (Willey et al., 2004). (b) Anthropogenic carbon inventory, based primarily on observations collected in the 1990s (Sabine, personal communication).

2.7.5. Heat and freshwater transport variations based on *in situ* data

Ocean heat and freshwater transports are calculated from either their air-sea fluxes or directly from in situ ocean observations of temperature, salinity and velocity. Annual global and full water column data sets of *in situ* properties, with requisite velocity analysis, are not possible. Global analyses are performed by research groups using various methods working with global data sets (Figure 2.7.17). These products are fully described in numerous research and review articles (e.g. Bryden and Imawaki, 2001; Wijffels, 2001; Ganachaud and Wunsch, 2003; Macdonald, 1998).

Seasonal to interannual variability in transports are products primarily of the high density XBT (VOS) network, usually combined with ongoing boundary current measurements and altimetry. This section of the report ideally should show the most recent time series of these calculations, variations in upper ocean temperature transports computed from XBT and altimetric data including estimates from 2003.

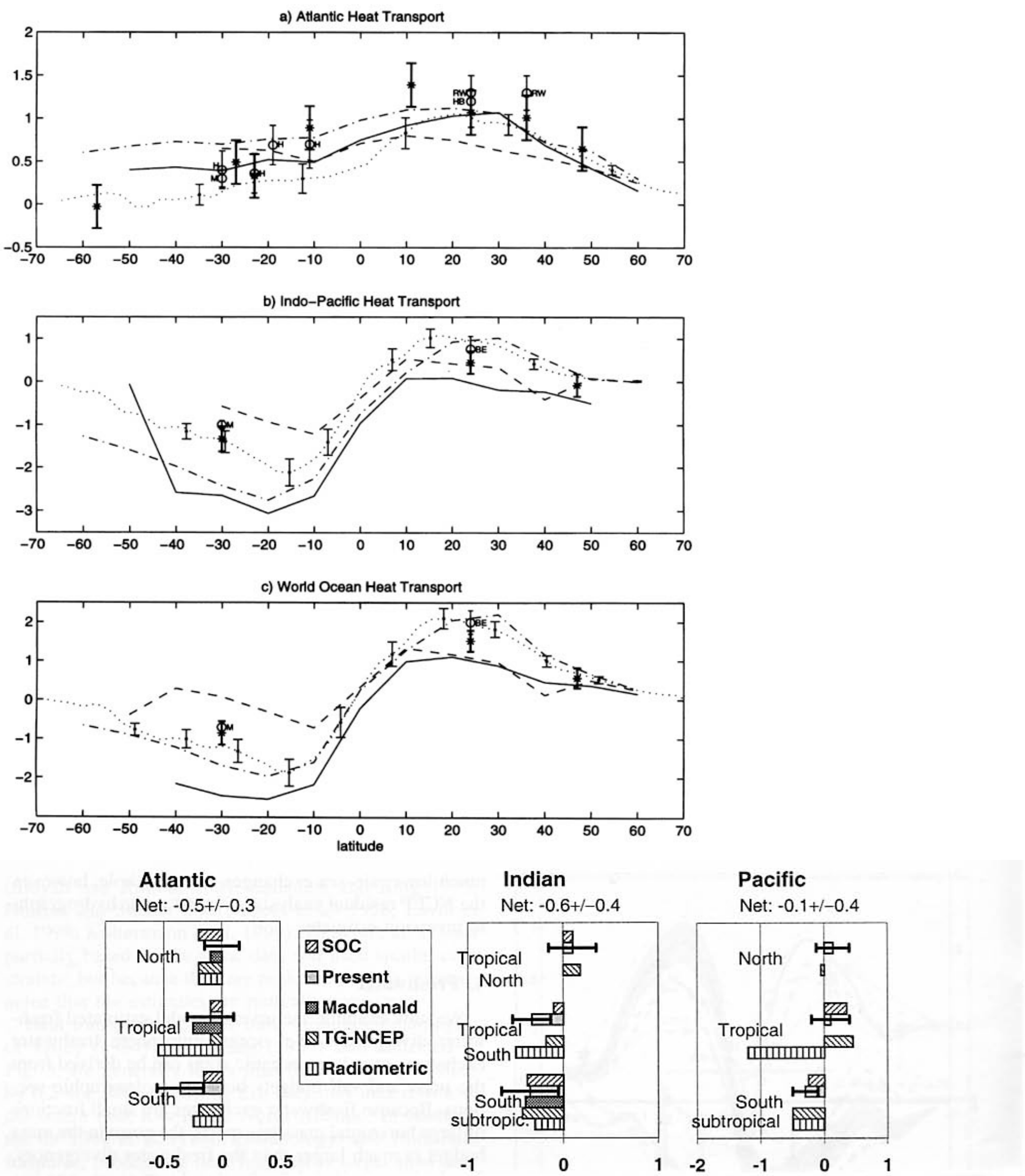

Figure 2.7.17. (a) Meridional heat transport estimates (PW) from Macdonald (1998), including a summary of earlier estimates. (b) Meridional freshwater divergence estimates (Sv) from Ganachaud and Wunsch (2003).

2.7.6. Summary of selected publications in 2003 dealing with ocean property variations prior to 2003

Since oceanographic data is often not reported or analyzed in real time, important comparisons of specific years with long-term means are often made several years later. This is particularly true for subsurface changes, and especially those involving salinity. Several publications in 2003 highlighted changes in the intermediate and deep ocean properties. A great deal of attention, including by the popular press, was given to observed freshening from the 1950s to the early 2000s in the mid-depth, mid-latitude North Atlantic and Norwegian Sea (Dickson et al. 2003, which incorporated some materials from Dickson et al., 2002; Curry et al. 2003). The freshening occurred through the top 1000 meters and was associated with an increase in low density upper ocean water (in the Norwegian Sea in Figure 2.7.18 from Dickson et al., 2003, their Figure 2) and throughout the northern North Atlantic (shown above in Figure 2.7.15).

Long-term temperature trends can also not be discerned easily in individual yearly data. Analysis of temperature trends at different depths and latitudes, using data-assimilating models continues the recognition based on subsurface float and hydrographic data of warming in the Southern Ocean (Gille, 2002).

2.7.A.1 Products and websites for 2.7
Global SST for 2003: http://www.cdc.noaa.gov/cgi-bin/db_search/SearchMenus.pl

NCEP monthly SST anomalies: http://www.emc.ncep.noaa.gov/research/cmb/sst_analysis/

Surface and subsurface temperature analyses (Pacific only): http://argo.kishou.go.jp/index.html

Surface to 400 m temperature, heat content: http://jedac.ucsd.edu

Surface salinity analyses (North Atlantic only):
http://www.met-office.gov.uk/research/ocean/operational/foam/realtime/index.htm

Subsurface salinity analyses (Atlantic only):
http://www.coriolis.eu.org/coriolis/cdc/atlantic_area.htm

NOAA CPC climate indices: http://www.cpc.ncep.noaa.gov/products/precip/CWlink/

NAO index: http://www.cgd.ucar.edu/~jhurrell/nao.stat.winter.html

NAO index: http://www.cru.uea.ac.uk/cru/climon/data/nao/

PDO index: http://tao.atmos.washington.edu/pdo/

Tropical Atlantic climate indices:
http://www.cpc.noaa.gov/products/analysis_monitoring/CDB_archive.html

Guide to Climate Data Sets: http://www.cgd.ucar.edu/cas/guide/

Wide range of data sets: http://www.usgodae.org

ARGO deployments and information: http://w3.jcommops.org

ARGO maps (Atlantic): http://www.coriolis.eu.org/coriolis/cdc/atlantic_area.htm

NOAA GFDL data portal: LAS/DODS format, 1980-present analyses
http://nomads.gfdl.noaa.gov

SST indices from the Climate Diagnostics Bulletin archive:
http://www.cpc.noaa.gov/products/analysis_monitoring/CDB_archive.html
Sea ice extent, concentration: http://www.jpl.nasa.gov/pictures/seaice

2.7.A.2 Comments on product availability

- Climate Diagnostics Bulletin has interesting information on a variety of climate phenomena, including tables of indices, but discussion is focused on ENSO. Need references for understanding the indices, and up-to-date interpretation.
- Climate Prediction Center also has interesting information - would be useful to have the predictions followed up on, and archived information easily available. Perhaps segued to the Climate Diagnostics Bulletin.
- No ARGO maps available for globe. Available products are from France and Japan, and are not presented as anomalies, but as actual (or assimilated actual) field. U.S. certainly should be producing such maps given the large U.S. investment in ARGO.
- Global salinity analyses for 2003 apparently not available. Presumably ARGO will be used to fill this gap in the future.
- Given large U.S. investment in VOS XBT measurements, should be more results out there for use, with associated analysis.
- Heat content maps available from JEDAC, but their SST maps did not match with the Reynolds SST maps, so not clear what to trust. Levitus product on annual basis would be great. Also upper ocean salt content and anomalies.
- (non-NOAA comment: NCAR data sets are not up to date - SST only until end of 2002, other oceanographic data sets end earlier.)

References

Alley, R. B., J. Marotzke, W. D. Nordhaus, J. T. Overpeck, D. M. Peteet, R. A. Pielke Jr., R. T. Pierrehumbert, P. B. Rhines, T. F. Stocker, L. D. Talley and J. M. Wallace, Abrupt Climate Change, *Science, 299,* 2005-2010, 2003.

Bryden, H. L. and S. Imawaki, *Ocean Heat Transport. Ocean Circulation & Climate*, G. Siedler, J. Church and J. Gould, Eds., Academic Press, 455-474, 2001.

Curry, R., R. R. Dickson and I. Yashayaev, Ocean evidence of a change in the fresh water balance of the Atlantic over the past four decades, *Nature, 426*, 826-829, 2003.

Dickson, R.R. et al., 2002.

Dickson, R. R., R. Curry and I. Yashayaev, Recent changes in the North Atlantic, *Philosophical Transactions of the Royal Society London A, 10.1098/rsta.2003, 1237*, 1917-1934, 2003.

Fetterer, F. and K. Knowles, Sea Ice Index. Boulder, CO: National Snow and Ice Data Center. Digital media, 2002.

Ganachaud, A., and C. Wunsch, xxx, *J. Phys. Oceanogr*., 16, xxx-xxx, 2003.

Gille, S., Warming of the Southern Ocean since the 1950s, *Science, 295*, 1275-1277, 2002.

Macdonald, A., The global ocean circulation: a hydrographic estimate and regional analysis, *Progress in Oceanography**,** 41*, 281-382, 1998.

Mantua, N. J., S. R. Hare, Y. Zhang, J. M. Wallace and R. C. Francis, A Pacific interdecadal climate oscillation with impacts on salmon production, *Bulletin of the American Meteorological Society, 78*, 1069-1079, 1997.

McPhaden, M. J., Evolution of the 2002-2003 El Niño, *Bulletin of the American Meteorological Society*, May, in press, 2004.

Molinari, R.L., R. A. Fine, W. D. Wilson, R.G. Curry, J. Abell and M. S. McCartney, The arrival of recently formed Labrador Sea Water in the Deep Western Boundary Current at 26.5-degrees-N. *Geophysical Research Letters*, 25, 2249-2252, 1998.

Reynolds, R. W., N. A. Rayner, T. M. Smith, D. C. Stokes and W. Wang, An improved *in situ* and satellite SST analysis for climate, *Journal of Climate, 15,* 1609-1625, 2002.

Saji, N. H., N. Goswami, P. N. Vinayachandran and T. Yamagata, A dipole mode in the tropical Indian Ocean, *Nature, 401*, 360-363, 1999.

Smith, T. M. and R. W. Reynolds, Extended Reconstruction of Global Sea Surface Temperatures Based on COADS Data (1854-1997), *Journal of Climate, 16*, 1495-1510, 2003.

Thompson, D. W. J. and J. M. Wallace, Annular modes in the extratropical circulation. Part I: Month-to-month variability, *Journal of Climate, 13*, 1000-1016, 2000.

Wijffels, S.E., *Ocean Transport of Fresh Water. Ocean Circulation & Climate*, G. Siedler, J. Church and J. Gould, Eds., Academic Press, 475-488, 2001.

Willey, D. A., R. A. Fine, R. E. Sonnerup, J. L. Bullister, W. M. Smethie and M. J. Warner, Global oceanic chlorofluorocarbon inventory, *Geophysical Research Letters*, *31*, L01303, doi:10.1029/2003GL018816, 2004.

Wunsch, C., What is the thermohaline circulation?, *Science, 298,* 1179-1181, 2002.

Zhang, Y., J. M. Wallace, and D. S. Battisti, ENSO-like interdecadal variability: 1900-93, *Journal of Climate, 10*, 1004-1020, 1997.

2.8 EL NINO AND HEAT CONTENT VARIATIONS

by Michael J. McPhaden, Pacific Marine Environmental Laboratory, Seattle, Washington
(Adapted from McPhaden, M. J., Evolution of the 2002-2003 El Niño, *Bulletin of the American Meteorological Society*, in press, 2003.)

El Niño Southern Oscillation (ENSO) variability is intimately linked to alternating stages of oceanic heat content build-up and discharge from equatorial latitudes. These heat content variations are mediated by wind-forced equatorial waves and affect sea surface temperature (SST) through equatorial upwelling and other processes. Changes in SST then feedback to the atmosphere to modify surface wind and precipitation patterns. The slow seasonal evolution of upper ocean heat content and its feedbacks to the atmosphere accounts for the characteristic interannual time scale of ENSO. The predictability of ENSO likewise derives from the deterministic wind-driven ocean dynamics that govern this slowly evolving upper ocean thermal field.

According to the "recharge" oscillator theory for ENSO: 1) a build-up of excess heat content along the equator is a prerequisite for the occurrence of El Niño; 2) the equatorial Pacific is purged of excess heat content during El Niño; and 3) the time between El Niños is determined in part by the time it takes to recharge equatorial latitudes with excess heat once again. Empirically it has also been determined that the magnitude of El Niño SST anomalies usually scales in proportion to the magnitude of the prior heat content build-up.

Zonally integrated heat content along the equator provides a convenient index for interpreting ENSO variability in terms of recharge oscillator theory. One definition of heat content for this purpose is the integrated warm water volume (WWV) above the 20°C isotherm between 5°N–5°S from the eastern to the western boundary of the Pacific. It is evident from the WWV time series and the NINO3.4 SST index (see Figure 1) that a build-up in heat content along the equator has preceded all El Niños since 1980 by 2–3 seasons. The heat content build-up prior to the 2002–03 El Niño was about half that prior to 1997–98, and comparable to that prior to the 1986–87 and 1991–92 El Niños. Based on this heat content precursor, one would have expected maximum NINO3.4 SST anomalies for the 2002–03 El Niño to be significantly smaller than those in 1997–98 and similar to those in 1986–87 and 1991–92.

WWV along the equator peaked in September 2002 after which it began to rapidly decrease, in accordance with the idea that El Niño should purge excess heat from the equatorial band. WWV became weakly negative in February–April 2003, consistent with the existence of a shallower than normal thermocline along the equator at that time. The steep plunge in WWV from September 2002 to February 2003 was a harbinger of the 2002-2003 El Niño's demise, though WWV subsequently rebounded to positive values in mid-2003 in response to renewed episodic westerly wind forcing (Figure 2). The persistence of this elevated WWV during the second half of 2003 is linked to slightly elevated El Niño-like SSTs in the equatorial Pacific that some forecast models indicate will persist into the Northern Hemisphere spring.

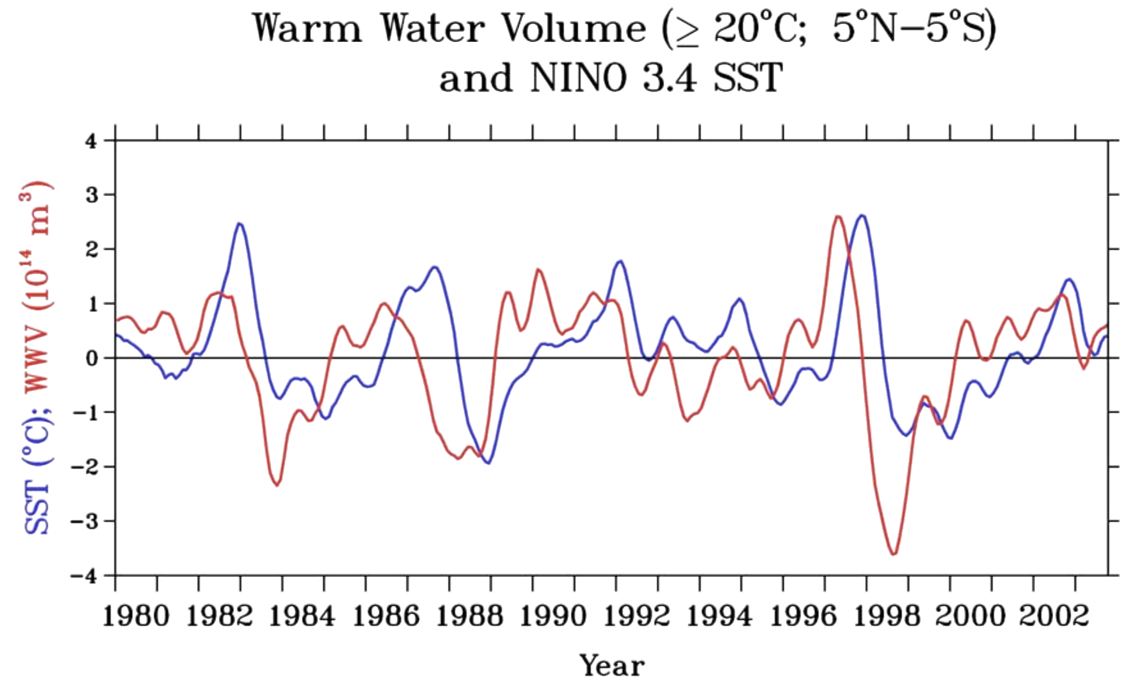

Figure 1. Monthly anomalies of warm water volume (5°N–5°S, 80°W–120°E above the 20°C isotherm) and NINO3.4 SST (5°N–5°S, 120°W–170°W) from January 1980 to December 2003. Warm water volume is based on a blended analysis of TAO/TRITON moored time series data and ship-of-opportunity expendable bathythermograph (XBT) data. Time series have been smoothed with a 5-month running mean filter for display.

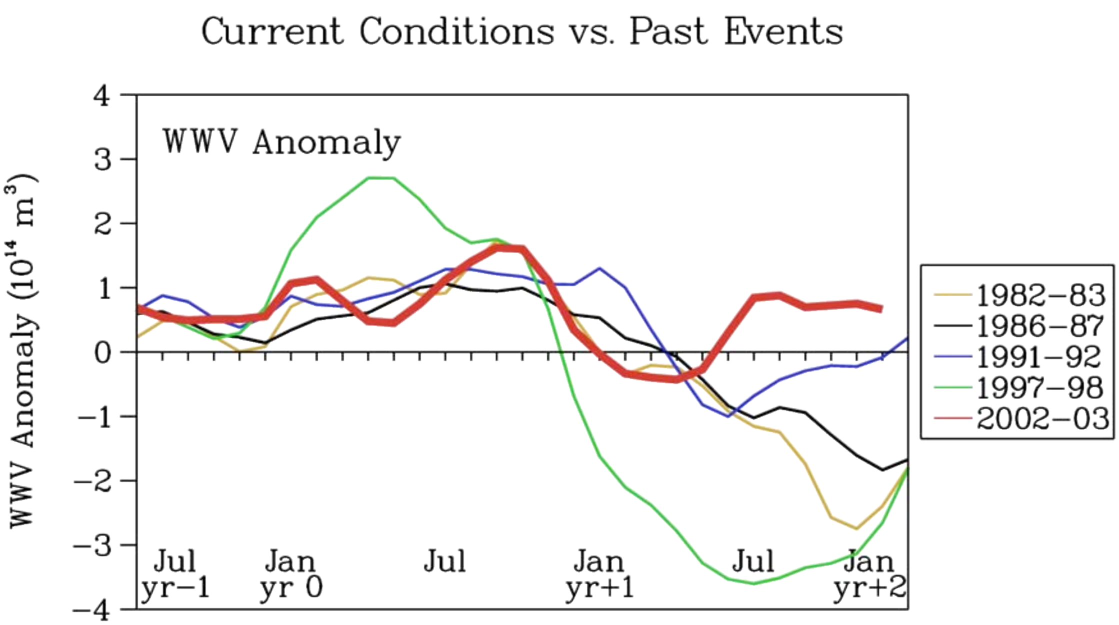

Figure 2. Monthly warm water volume (WWV) variations in the Pacific during El Niños since 1980, starting in July the year before each El Niño and ending in January the year after.